ACOUSTIC EMISSION MONITORING
ON FIBER REINFORCED BRIDGE PANELS

by

JAMES CHRISTOPHER FLANNIGAN

B.S., Kansas State University, 2005

A REPORT

submitted in partial fulfillment of the requirements for the degree

MASTER OF SCIENCE

Department of Mechanical Engineering
College of Engineering

KANSAS STATE UNIVERSITY
Manhattan, Kansas

2008

Approved by:

Major Professor
Youqi Wang

Abstract

Two fiber reinforced polymer (FRP) bridge deck specimens were analyzed by means of acoustic emission (AE) monitoring during a series of loading cycles performed at various locations on the composite sandwich panels' surfaces. These panels were subjected to loads that were intended to test their structural response and characteristics without exposing them to a failure scenario. This allowed the sensors to record multiple data sets without fear of having to be placed on multiple panels that could have various characteristics that alter the signals recorded.

The objective throughout the analysis ias to determine how the acoustic signals respond to loading cycles and various events can affect the acoustical data. In the process of performing this examination several steps were taken including threshold application, data collection, and sensor location analysis. The thresholds are important for lowering the size of the files containing the data, while keeping important information that could determine structurally significant information. Equally important is figuring out where and how the sensors should be placed on the panels in the first place in relation to other sensors, panel features and supporting beams.

The data was subjected to analysis involving the response to applied loads, joint effects and failure analysis. Using previously developed techniques the information gathered was also analyzed in terms of what type of failure could be occurring within the structure itself. This somewhat aided in the analysis after an unplanned failure event occurred to determine what cause or causes might have lead to the occurrence.

The basic analyses were separated into four sets, starting with the basic analysis to determine basic correlations to the loads applied. This was followed by joint and sensor location analyses, both of which took place using a two panel setup. The last set was created upon matrix failure of the panel and the subsequent investigation.

Keywords: acoustic emission (AE), fiber reinforced polymer (FRP), composite, sandwich panel, analysis, general analysis, location analysis, joint analysis, acoustic analysis, failure analysis, matrix failure, sensor data collection.

Table of Contents

List of Figures

Acknowledgements

Many people have been important in the development and completion of this project and I'd like to take this opportunity to immortally recognize their help and support.

I would first and foremost like to thank Professor Youqi Wang, graduate advisor and major professor of my committee, for her guidance, encouragement and especially her patience with me throughout this process; Professors Kevin Lease and Sameer Madanshetty for serving as members of my committee and always being willing to answer questions or listen to concerns about anything.

Next, I would like to thank the MNE department at K-State for their help in each aspect of my education and development, especially Department Head Mo Hosni, and members of the staff: Erin, Sherry, Carol, Marcia, and Jason; the people who helped perform the testing for the project, namely Engineer Dave Meggers of the Kansas Department of Transportation, and his assistant Travis Hirt; all involved in the creation of the earlier papers and projects, especially Richard Gostautas, who was able to help in several ways, including setting up our monitoring device.

Also special thanks to Kansas Structural Composites for creating and providing the FRP panels; Physical Acoustics for building the monitoring device; KDOT for sponsoring the research.

Finally, I'd like to thank my parents, Susan and Richard for their constant encouragement; my siblings, Tommy and Jennifer for helping me relax and keep things in perspective; Dotty & John and Lois & Thomas for the various things they've each taught me; my close friends for not taking it personally when I couldn't be there, and showing me support.

CHAPTER 1 INTRODUCTION

Interest in using fiber-reinforced polymer (FRP) as a highway bridging material began in 1970's China, with the goal of building large span, two-lane bridges. After much research and development the world saw its first composite bridge deck built in Beijing, China in 1982. [Feng, 2006] However, following this milestone in bridge design and construction, the use of composites as a serious bridging material went primarily undeveloped and no new structures are known to have been built for over a decade.

In 1993 the western-world saw its first advanced composite bridge built in Aberfeldy, Perth and Kinross, Scotland with decks and structural towers constructed out of E-Glass fiber material, while the support cables were made of Kevlar-49 material. These two uses resulted in not only a composite bridge, but the first to employ multiple types of composite materials in the design. [BRE, 2001] However, while it met all the criteria for being a traffic bridge, this should be taken lightly as it was only built to serve as a footbridge, limited to pedestrian use at the city's local golf club. The next bridge designed to carry automotive traffic is called The Bonds Mill Lift Bridge located in Stonehouse, England. While it is not a long bridge it was the first FRP bridge outside China built specifically for vehicular traffic and is not a conventionally designed static bridge, but is instead designed as a bascule-style bridge that does not impede the active water- route it passes over. However, the overall capabilities of this structure are somewhat limited, as only a single lane of traffic is able to travel at a time and it is constantly monitored due to its untested type of material to insure safety. [McWilliam, 2004]

The first FRP Bridge in the United States, and first in the western hemisphere to allow free flows of two-lane traffic, was built by Kansas Structural Composites Inc. (KSCI) in 1996 to cross No-Name Creek near Russell, Kansas. While not technically the first bridge of its kind, the advancements in design and the material's relatively new type of construction won it overwhelming praise from a variety of sources. Organizations ranging from the scientific community to the media broadcasters quickly praised it as one of the biggest advancements of its kind in several years. The accolades included the awarding of both 'Best of Market' and the prestigious 'Counterpoise Grand Design Award' from the International Composite Expo held in January of 1997, as well as being recognized at The R&D 100 Awards for being one of the most important developments made that year. The bridge can be seen in the following figure. [KSCI, 2007]

Figure 1-1 No-Name Creek FRP Bridge (Original Source: KSCI.com)

Since installation and construction of the No-Name Creek bridge several other bridges have been built by KSCI in a variety of locations. While a majority of these are in Kansas nearly a dozen are in other states, including Missouri, New York, and West Virginia. Several other companies have started up similar construction methods in this time period as well, resulting in possibly hundreds of FRP bridges across the country. The reasons for this increased interest in this construction method are numerous, and while some could be a simple response to civic and state governments simply wanting a new and unique structure, there are more than enough advantages to merit construction of an FRP bridge.

Fiber-reinforced polymer bridges can be installed in a relatively short amount of time. The structure itself is built at a controlled facility separate from the onsite location making it easier to control the fabrication process as well as create parts that might be impossible to do at the construction location due to area constraints of machinery availability. Because much of the process occurs before the main construction begins the composite material is given time to cure and become usable as a solid panel for the bridge decks. The quick onsite installation was able to make the entire construction time of the No-Name Creek Bridge only a single day from start to finish. Adding to the ease and quickness of the construction is the relative lightness of the FRP panels in comparison to other materials, such as concrete, steel and wood.

The decrease in panel weight also relieves much of the stress experienced by the support structure. When bridges are constructed a large percentage of the structure is already needed to simply keep the panels in place, this can be an arduous task when the panels themselves create a large portion of the weight experienced by the structure. However, FRP panels are designed to hold a large load while remaining relatively light and the resulting lower panel load subsequently creates a large difference between what is and can be loaded, increasing in the amount of traffic load that can be placed on the bridge.

Repairs are also capable with FRP panels if the need should arise. If there is a possibility the bridge will need widened in the future the initial installation can be performed in a way to allow the panels to be removed and new, larger ones, installed quickly. The new panels can take advantage of the pre-existing support structure as well, resulting in only hours of actual construction taking place. Of course if a panel fails or starts showing signs of impending failure it could also be replaced with another panel in a short amount of time. [KSCI, 2007]

At the time of implementation, the No-Name Creek Bridge was new and experimental, without much previous analysis; an idea that required early research and analyses to be performed to verify it’s abilities for future installations. To do this a collaborative effort was initiated between Kansas State University and KSCI to determine what effects large forces have on the panels and material properties by performing both in-lab and field tests. The lab tests consisted of both small scale and full scale panel tests using static loads to record the bending properties of the material. Upon completion of the bridge further examinations were performed several times; once after installation, after one year of service and after eight years of service. The post-installation analyses consisted of static loads applied by use of a dump truck at the center of each panel, slow-speed static tests and high-speed dynamic tests in which the truck was driven over the bridge. After eight years the tests reported that no noticeable change had occurred in the bridge rigidity properties and was not effected by environmental decay. [Zhou, 2007]

Another test was conducted over the course of a year that consisted of a monitoring device measuring the temperature of the FRP panels at various points and the overall deflection of the panels. The initial analysis of this bridge was carried out by using thermal and deflection monitoring techniques to examine local climate impact on the structure over a year. The results showed that over the course of the year and days the panels follow a cyclic deflection pattern indicating that the temperature changes have a dramatic effect on the curvature of the panels. As a result there was a concern of possible delamination and eventual panel failure due to bending effects. [Liu, 2006]

During this time a set of bridges had been installed by the Kansas Department of Transportation (KDOT) in 1999 to replaced two state highway bridges that had deteriorated to a point at which the decks faced possible collapse. In the course of replacing the panels, the decision was made to widen the bridge and replace the entire deck structure with fiber-reinforced polymers. [KSCI, 2007] Over time the FRP panels began to delaminate between the outer sheet of material and the primary core structure. The primary cause of this occurrence is believed to have been due to the thin, flat outer material, and its inability to completely bond with the core material. In Figure 1-2 below the delamination occurrence between layers is quite visible upon panel removal. To fix this problem the outer material was replaced with a three-layer chop-mat fiber that created a better hold and has now been in service for several years without any known problems. [D. Meggers, interview, 2008]

Figure 1-2 Material delamination in bridge panel (Original Source: D. Meggers)

Due to the possibility of the material experiencing fiber breakage or delamination it was decided that a system should be developed to monitor bridges in case this would be to ever happen. A method was sought to help understand the failure mechanisms experienced by the panels when critical loads are reached. From this information it might be possible to determine where and when a failure would occur based on sudden events and changes that happen prior to a critical break. The use of non-destructive tests (NDTs) offered highly attractive options as they will allow for monitoring of the structure while allowing the bridge to be in use. The technique decided on was Acoustic Emissions (AE) monitoring. This will take advantage of the sound created when a fiber breaks, layers delaminate or other types of failures occur in most composite materials before larger failures occurs. Use of this method would not require a person to be constantly present to monitor the site, and the analyzing itself can be carried out in a variety of ways, including periodic testing or continuous monitoring, allowing year-round analysis of acoustic signals and development of possible warning signs of failure.

For a proper monitoring system a series of analyses need to be conducted to determine the proper application of AE in reference to the current project. The following points were identified as needing to be analyzed and understood before implementation of the AE monitoring device can be properly used:

1. The relationships, if any, between loading damage and the acoustic emissions detected by the sensing equipment.
2. If and what thresholds should be applied to the equipment to record data that is important for the analysis procedure while removing background and environmental noise.
3. Determine the range that should be used for the sensors in terms of the area each can cover functionally and the distance each can be placed from each other.
4. Possible sensor arrangements and placement constraints that should be used in future analyses.
5. Possible sensor layout for a long term monitoring analysis.

CHAPTER 2 BACKGROUND REVIEW

The possible applications for acoustic emissions is obvious in the field of bridge structures, and there are many possibilities within the field of composite structures, which looks poised to be used in a much larger scale in the near future. However, an explanation as to what an acoustic emission actually is still hasn't been discussed or defined in this report. A quick look at the history and development of acoustic emission monitoring, as well as related modern uses would help explain what is being discussed. It is important to examine what exactly these emissions are, as well as get a brief look into the history behind this subject and how it developed into what it is today. In this section the development of past uses and some current applications of acoustic emission monitoring will be presented to explain the background of acoustic emissions and where it could be used in the future.

2.1 What is Acoustic Emission Monitoring

A basic and widely accepted definition of Acoustic Emission (AE) monitoring is the detection of transient mechanical waves in a source material. These waves are usually formed when a sudden change in strain takes place in a localized point by any of several possible methods. This means that when a crack or other flaw in a material creates some change in the overall material, usually through growth, there are waves formed that can be recorded and analyzed, as shown in Figure 2-1.

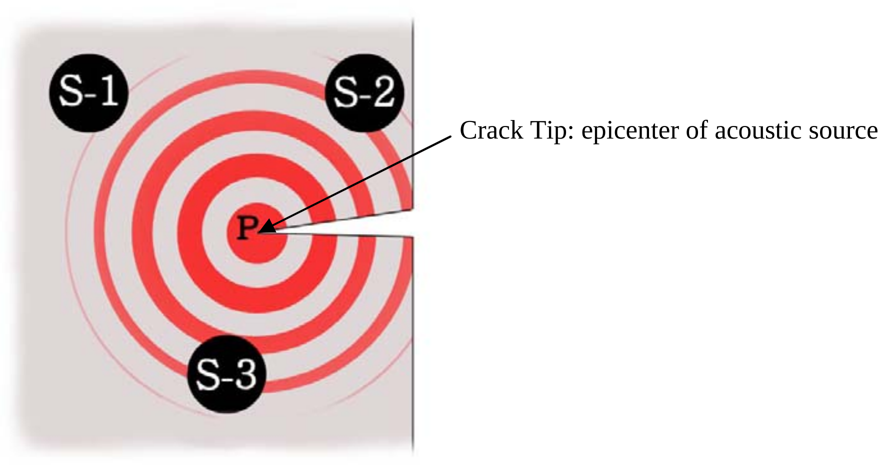

Figure 2-1 Acoustic wave propagation from failure point, P, to three sensor locations: S-1, 2, 3.

Based upon this same figure it can be seen that the locations of the sensors are important, as the closer the failure epicenter, point P, is to the monitoring device the stronger the signal is. This gives the user an ability to locate the point of failure to some degree by use of triangulation methods.

A great natural example of how modern AE works is by examining the propagation of an earthquake. In and around a fault line forces and stress are being built up over time. At some point the tension becomes too much and there is a sudden shift of the ground structure, whether on the surface or subterranean does not matter. When this event happens the released energy is distributed in sudden waves propagating out from the epicenter, resulting in large tremors. These waves are then used to determine the strength, location, and even the type of event that created the quake. This is the basic principle to AE monitoring; it simply happens on a smaller scale.

Origin of Acoustic Emission Monitoring

The use of the AE monitoring method has been around for over half a century, but it hasn't been until the last few decades that it has truly expanded and come to be seen as a serous structural monitoring technique.

Acoustic emissions have been used for centuries by many civilizations in many parts of the world. Some of the earliest examples known are earthquakes, as mentioned earlier, and in mining practices. Workers in a mine shaft can often time get some warning of an impending event by listening to or feel rumbling in a shaft. Often time the sound can be heard before a cave in and are used as an alert that people should get out or take cover before a possible collapse occurs.

The first detected acoustic signals that were also recorded for analysis occurred during a study by a Japanese timber miner named Kishinoue. In 1934 he developed a method of recording the acoustic emissions created during bending tests of quarter-sawn wood beams. "He transferred the vibrations (AEs) associated with the fractures of a board into an electronic gramophone through a needle on the board." The vibrating needle would create marks on cinematographic film that could be further inspected for AE events that took place during the bending tests [Kawamoto, 2003]. While this method was used to determine the strength of trees that had been cut down, a quite different method of AE monitoring was being developed in Germany to record their growth.

A man by the name of Forster was analyzing sounds coming from plants in Germany, but not for structural purposes. Instead he noticed sounds created while the plant was growing and wanted to record the AE for further study. In order to do this he developed a system that would measure the small voltage changes created whenever resistance changed in his recording device due to the sound wave passing through a strain sensitive material. This method, while used long ago, is basically the same as the current one employed by most of the world's AE monitoring devices. [Kawamoto, 2003]

Monitors today are a combination of many components that work together to record the desired data; however, the majority of these pieces can be condensed into two parts. The first is the acoustic sensor itself. Even though these devices are small they are also very important to the device as a whole, as without them there would be no data. The sensors are actually a form of transducer, and are attached directly to the material being analyzed. Transducers function by converting the mechanical waves in the material into an electrical signal by using a special material called a piezoelectric crystal, or sometimes simply a Piezo. This material has the ability to generate an electric voltage when a stress is applied, creating a natural way to record small changes in a material's surface stress easily. When an acoustic wave is created the compressions and tensions created can be picked up by the sensor and in turn the crystal material inside, creating an electric signal that can be recorded by the data acquisition system for further analysis.

The second main part is the Data Acquisition System (DAQ) or computer processor. Due to sophisticated DAQs, modern AE monitor can be self-sustained upon activation if given a proper power source and the correct information to perform the desired tasks. Most systems can be set up to monitor and record the data until the user wants the data to be sent remotely to a predetermined computer or FTP site for analysis. The DAQ is also responsible for applying any thresholds deemed necessary to the project or get rid of unwanted noise.

The sensors can come in a variety of shapes and styles, which can be picked specifically for the analysis needed. One of the most common options available is the frequency range of the desired sensor. The choice of sensor frequency comes with benefits and drawbacks regardless of which option is chosen for the project. This is due to the nature of the acoustic waves; where a high frequency wave will be very sensitive to acoustic events but typically do not have a large sensor range, leaving the sensor's abilities limited. In this project a sensor was chosen with a low frequency due to the large size of the structure being monitored and the amount of devices being used. However, an additional drawback in using a low frequency sensor is the effect of environmental and background noise, creating more data that will need to be filtered out.

Benefits of Acoustic Emission Monitoring

The first and possibly most important benefit to using AE monitoring is that it is a Non-Destructive Test (NDT) that can be performed on a variety of materials and geometries without needing to remove them from service or otherwise harm them. This however cannot be the only consideration; there are many other NDT methods available including the following:

- Electromagnetic Testing (ET)
- Radiographic Testing (RT)
- Ultrasonic testing (UT)

If we compare the methods above they are all able to detect defects within a material; however, upon a further comparison of the techniques only one stands out as being suitable for the needs of this project. The first option, Electromagnetic, is composed of several possible processes that involve creating an electric-magnetic field or current within an object. The results can be analyzed and used to determine if there is a defect within the material by examination of how the field of current travels through the volume under observation. This testing process is used heavily in piping and tube manufacturing as it is able to be used proficiently on metallic materials such as steels and some irons. Due to the need for an electric or magnetic field creation in the material, it is virtually impossible to use on the FRP materials and not considered a possible technique.

The next method listed, Radiographic, uses short wavelength radiation by means of using high energy photons, or in some cases neutrons, to determine what is occurring in the structure. Unlike ET this form of testing is not dependent on the conductivity of the material, and the signal can pass through most materials without much difficulty. The amount of the radiated beam that passes through a structure can be collected and analyzed to determine how much was stopped or reflected away. This data can then be used to determine where and what kinds of defects are occurring within the observed part. The process has two major drawbacks in its general use however, design and safety. The design of RT apparatuses makes them either too large or too easy to damage when placed in an open environment. Another issue with the design is the general use, where a transmitter and receiver are needed on either side of the structure, or in our case on top and bottom of the panels. While this would be fine if no one ever wanted to use the bridge, this most likely will not occur and would therefore not be possible. The parts could be placed on either side of the panels with a decrease in the accuracy of the results, but the second problem still persists, safety concerns. The use of this NDT still creates radiation that could potentially endanger pedestrians or the environment surrounding the bridge. Because of these unwanted risks there is only one alternative to AE monitoring left to consider, UT.

These two similar methods both use sound waves in order to gather information about possible failures in the material. However, the ultrasonic method is an active system, while AE is passive, in that it creates a signal to travel through the material to find cracks and defects in a material. Ultrasonic Testing involves the use of a transducer that creates a high frequency sound wave that can be used to detect flaws by either reflection or attenuation methods. With the reflection technique the wave passes through the material until striking a flaw or other change in the material structure and is reflected back to the source. This method is similar to sonar in that it uses an echo-location technique, but is dissimilar in regard to the linearity of the device use. As the transducer is moved across the surface of an object with a gel or oil couplant, the sound is focused in a linear direction, meaning that it only detects what features are directly in front of the transducer. The second attenuation method has a source and reception sensor that produces the sound wave and detects what parts of the wave makes it through the material on the other side, respectively. This method creates another situation in which the monitoring is only occurring between two points on the structure and does not monitor for the creation of failure points and does little to determine if or how fast they are growing.

The passive AE system does not send a wave to detect cracks; rather it detects the crack's own sound waves. As the crack grows it usually will make a noise that can be detected by the AE monitoring system and in turn can be used to determine where the source is, if it is growing, and how quickly. If used properly this method can neglect unimportant defects while the bigger ones are constantly monitored regardless of direction from the sensors increasing the abilities and range of options in how the analysis should be conducted.

The many benefits and abilities inherent in AE is why it has been chosen as the medium to monitor the FRP bridges here, as well as many other tests performed across the globe. As discussed, the emergence of AE technology has shown to be very useful as a way to monitor structures both alone and as a compliment to other more classical testing and analysis methods.

Due to the wide applicability of its use AE has been used in a variety of industries to perform numerous jobs. Some of the industries that have made developments and use of AE are the petroleum, aerospace, nuclear, and transportation industries. Some of the uses of AE in research are related to determining the properties of various pressure vessels, dams, toxic waste reservoirs, and of course bridge structures.

2.2 Acoustic Emission Monitoring on Classic Bridge Structures

While AE monitoring devices have been employed on a wide variety of structures in many industries, one of the most significant in terms of this research is that of contemporary bridge structures. In the United States alone there have been many applications of this technology in a number of locations and climates where AE has been found to be an effective method.

The British Ministry of Defense performed what is considered the first true use of acoustic emission monitoring on a bridge in 1971 when two researchers named Pollock and Smith demonstrated that the data from the sensors, as well as from other collection devices showed a correlation with several results from other testing methods. This first analysis was critical for the future use of AE monitoring in that it showed that with enough work the acoustic monitors could be used to determine what events are taking place in the bridge without the use of other testing procedures. [Sison, 1996]

In the year after the initial project several other groups in the US performed their own tests and while successful in determining a correlation as well, they found that a problem did exist in the amount of noise that is also recorded by the equipment. However, this problem would be identified in the following decade as being due to the vibrations caused by vehicular traffic and in some cases environmental activity. [Sison, 1996]

In the 1970's the Federal Highway Administration (FHWA) made another development in the evolution of the long term monitoring system. It was during this time that the first battery powered devices were designed and tested, resulting in the ability to place the systems in locations previously unobtainable due to power availability constraints. A self supported memory system was also initiated, increasing the data recording possibilities. Now the system could both be placed anywhere and have a possibly longer recording time before the need for a user to get the memory from the system for analysis. [Sison, 1996]

Soon after these leaps were made in the collection of the data, a renewed interest occurred in the 1980's in the meaning of the data directly. A variety of researchers looked at the various components of the AE results, as well as the bridges the data were gathered from. The various projects included the identification of various types of events from the data recorded, the effects of traffic on the signal and the noise created, and the effects of the bridge materials on the overall acoustic signal. From these projects a series of thresholds could be applied that would help alleviate the noise effects and record only the desired noise related to 'un-natural' events. [Sison, 1996]

While in use, a traditionally built bridge is subjected to a variety of sounds from traffic, pedestrians, the environment and general background noise. In order to evaluate the ability of AE to properly monitor a steel bridge, Transportation Technology Center, Inc. performed a test to monitor cracks and crack growth in steel bridges. The results showed that background noise could be ignored successfully; crack initiation and growth was still able to be detected by examining the hit rate. [Uppal, 2000]

Since the inception back in the 1970's AE monitoring has developed into a reliable and heavily used monitoring tool on both small rural bridges and large highway bridges, including giant suspension bridges. Departments of Transportation in both Wisconsin (WIDOT) and California (CADOT) have used this technique on multiple highway bridges and successfully located possible failure locations during their application [Prine, 1995]

The Texas DOT applies AE sensors to many of its bridges, including the Fred Hartman Bridge shown on the next page in Figure 2-2. The bridge was officially opened in 1995, and is responsible for carrying State Highway 146 over the Houston Ship Channel. However, it was soon discovered that large oscillations occur on the stay-cables and through visual inspection the cables were creating cracks in the welds between the fixture holding the cables and the rest of the superstructure. In order to monitor the situation it was decided that a fatigue examination of an AE device with four sensors, supplemented by strain gauge monitoring, would be conducted at the Ferguson Lab at the University of Texas on a similar cable specimen. [Kowalik]

Figure 2-2 Fred Hartman Bridge (Source: Bayareahouston.com)

During the study it was determined that there were several breaks at the anchor and near the loading end. In all cases the breaks were found within the section of cable expected or in a section next to it. Since 2002 the Fred Hartman Bridge has had three acoustic sensors on each of the 192 cables monitoring at a near constant rate. The data is also filtered in the main Data Acquisition System in order to expel background noises and sends the information to a central processing unit where it can be categorized and uploaded to an online resource to be downloaded when needed. [Kowalik]

2.3 Acoustic Emission Monitoring in Composites

Acoustic Emission monitoring has been studied in a variety of ways in conjunction to its possible use on composite materials and as FRP seems to have branched off of the field of composites, many studies from each area can be applied to one another.

Acoustic Emission monitoring on composites has been around for over a decade and is constantly being developed by scientists and researchers for practical use in a variety of fields. Research has been heavily sponsored by NASA to study the use of AE on composite materials in various environments and conditions. Due to this sponsorship, it was determined that the extreme cold and conditions of space were most likely not be detrimental to the AE sensors as initially suspected by some, and they were able to perform their duty accurately upon reaching a temperature equilibrium with their environments. [Walker, 1997] This and other projects have shown that AE monitoring has the ability to monitor composites reliably even in harsh environments.

However, being able to record and analyzing data are two different things. If the data received is unable to be understood by the researcher, there is no point in the monitoring in the first place. Luckily the AE technique has been somewhat studied in its use on composite panels for some time and has been understood enough to determine if there is a problem and possibly where it is located.

To help understand the acoustic relationships some researchers have performed some experiments in which a cut was applied to the specimen so the failure source location could be easily controlled and monitored. The results showed that failures cause both high and low amplitude emissions; it just depends on the type of failure; longitudinal splitting by matrix failure or fiber fracture. In the tests performed by Thomas Ely, the analysis determined that the amplitude data could be divided into two bands divided at 60 dB. While subject to interpretation, the possibility that two failure types produced noticeably different data in terms of amplitude was an interesting development.” [Ely, 1996]

Indeed it appears that the lower amplitude and energy sources were closely linked to the longitudinal splitting, while the higher valued ones came from the fiber breaking. This is further supported by the lack of event buildup before the longitudinal failures; while it was certainly present before the fiber failure. This would be expected as in typical composite tensile tests sounds can be heard simply by the human ear moments before fiber breaks, but usually not as much before matrix failure. Another reason that gives support to this is that upon thinking about it, one would expect a fiber break to result in higher energy events due to the larger stress build-up that has occurred in relation to a matrix material.

CHAPTER 3 EXPERIMENTAL METHOD & ANALYSIS

Development of a monitoring system for Fiber Reinforced Polymer (FRP) bridge panels is the central focus of this research. Earlier projects performed at Kansas State University examined the thermal effects on a FRP bridge located outside Russell, Kansas in addition to developing a possible repairing technique for panels that did experience failure. These findings lead to the need of a method that can accurately determine the deterioration of the bridge by various methods, including fiber breakage and delamination [Liu].

3.1 Project stage background

The overall acoustic emission project has consisted thus far of two stages conducted by individuals at both the University of Kansas and Kansas State University. The first stage was performed by Richard Gostautus at University of Kansas and consisted of determining if acoustic sensors would be capable of detecting the failures experienced by the panels in controlled tests. Another element examined was how the acoustic emissions changed with the application and removal of loads [Gostautus, 2005].

To do this a set of five sensors were attached to a series of panels, widths varying between 6 and 30 inches, during bending tests that included failure examinations. Two sensors were attached to the top, two on the sides and one on the bottom during each testing session. The tests consisted of an application and partial removal of load at the center of the beam by use of an I-beam oriented perpendicular to the panel length. The early examinations had to do in part with determining the Felicity Ratio, the value corresponding to the Kaiser Effect in the FRP panels. Kaiser Effect is a trend related to acoustic emission, where the acoustics are recorded during load application, and partial removal. When the force is reapplied, the acoustic readings do not initially start up again. Instead the emissions do not occur until a particular stress is obtained at some fraction of the originally applied load's maximum value. A general graph of the loading cycle used during this analysis is shown in Figure 3-1 on the next page [Gostautus, 2005].

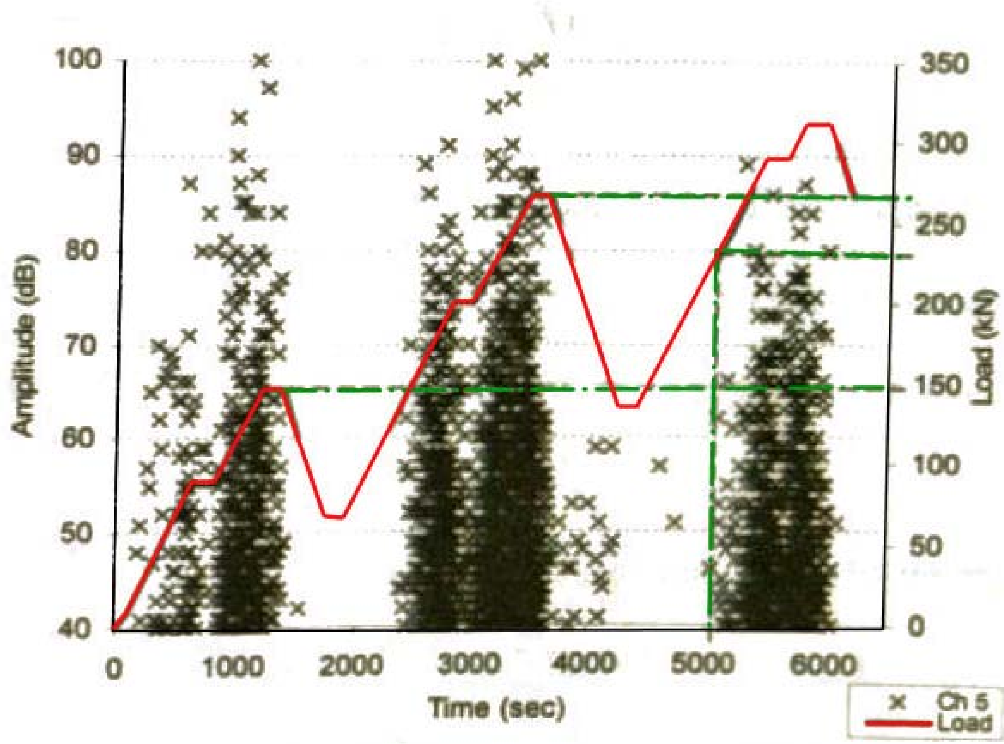

Figure 3-1 Load application in Keiser Effect analysis. (Original Source: Gostautus)

From examining the Keiser Effect it was demonstrated that the emissions recorded occurred when the loads were being increased and occurred more often after the previous maximum loading peak was approached. This outcome would be expected, as an increase in the load would infer an increase in the stress of the panel, as well as the fibers and matrix within it. In order for the material to remain unbroken, they would have to be able to support a stress equal to that experienced in earlier peaks, and would therefore not fracture until a higher load was applied [Gostautus, 2005].

The second analysis performed has to do with the ability to determine what properties are related to and occur during a panel's failure. Gostautus concluded that a graph of zones developed earlier could be used to aide in the classification of the type of failure being seen during the analyses, but several of these areas overlap making it difficult to classify all failures into a specific type. A general layout of the Amplitude-Duration Zone chart in comparison to data collected during one of his tests is shown in Figure 3-2 [Gostautus, 2005].

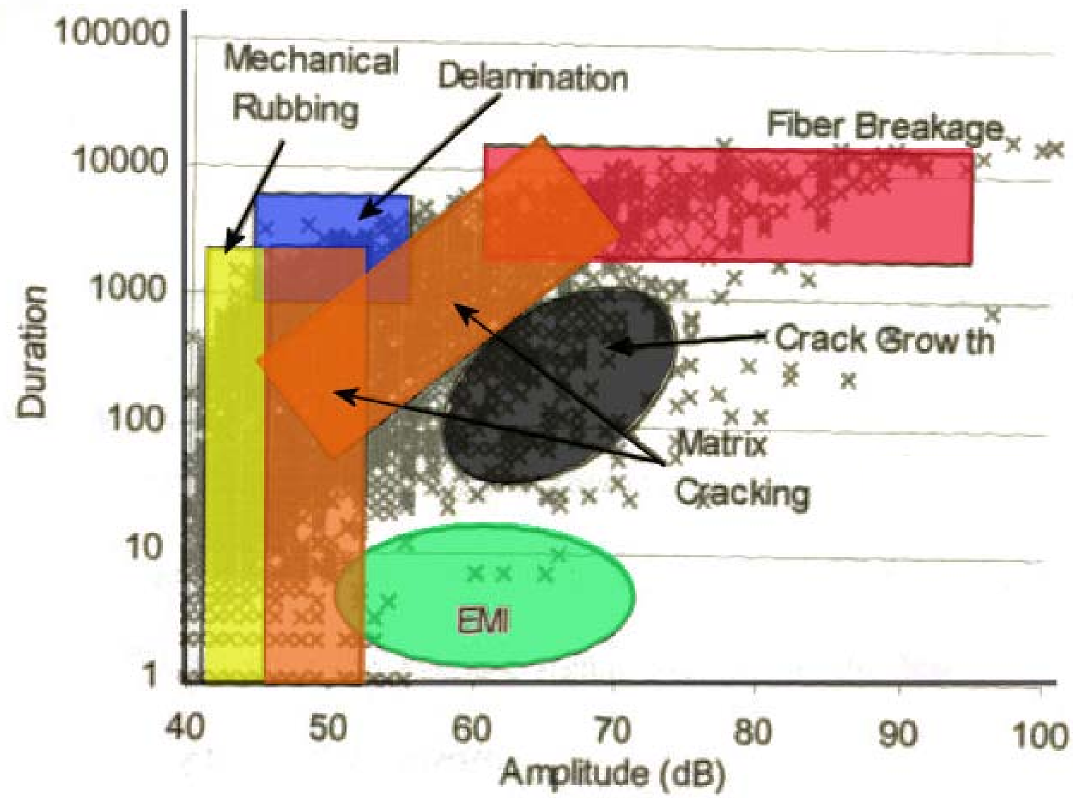

Figure 3-2 Cross Plot of Duration versus Amplitude. (Original Source: Gostautus)

One of the last areas examined had to do with the repairing of FRP panels and retesting the structure. Upon failure, the panels would be repaired by placing an outer wrapping on the structure and retesting it to determine if the structure is reusable. The determination was that the previously failed and repaired specimens were able to carry a larger load without failure while creating more acoustic noise recorded. The overall determinations of this stage of analysis determined the acoustic tendencies of the overall structure and examined how, by use of a linear technique, a failure location might be determined when between two sensors [Gostautus, 2005].

In the second stage, discussed in this paper, the analysis will be on the use of a network of acoustic emission sensors to determine the failure type and location. In addition this research looks at the transfer of an AE wave between two panels, further analysis of noise distribution and initial design set-up for a long term monitoring system is performed.

3.2 Equipment and Software

Equipment

Hardware able to handle multiple devices and apply a variety of user defined constraints, while maintaining a quick rate of data collection from the sensors is the central method being used for the sensor network analysis. The Sensor Highway II Data Collector (SH-II DC) was built by Physical Acoustics Corporation (PAC) and designed specifically for the current and future needs of the overarching project. It was designed to provide the most functionality while maintaining an easy operational setup and having the ability to work for a variety of setups.

The SH-II DC system is a data acquisition module comprised of many individual components. The overall DC is located within its own enclosure, protecting it from the environment and allowing all the parts to be in a controlled, safe space regardless of local weather conditions. The complete enclosed system and the Dell Laptop PC used to communicate with the system in this project can be seen below in Figure 3-3.

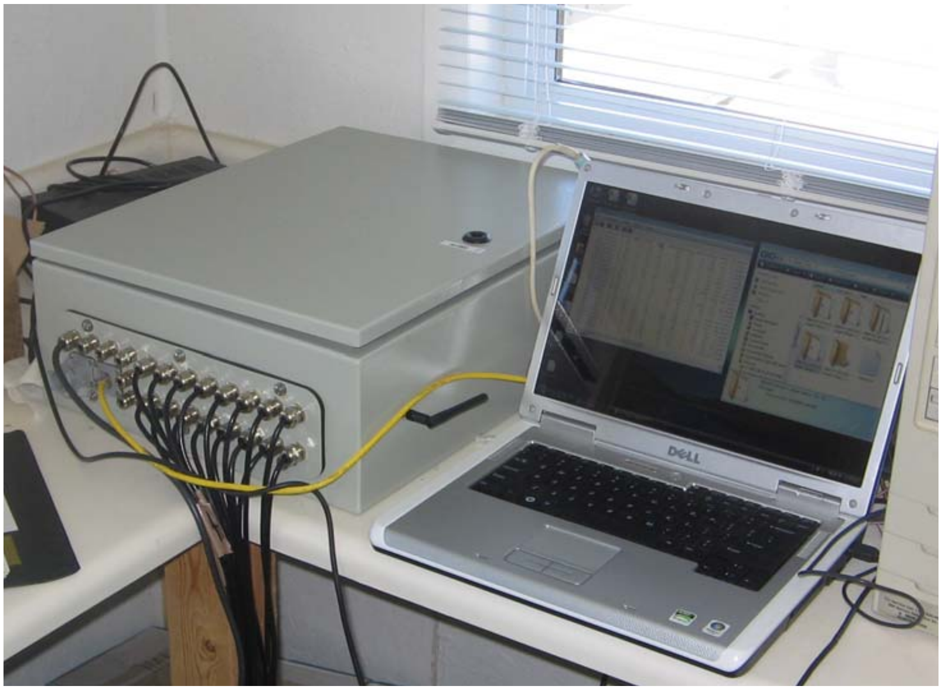

Figure 3-3 System Enclosure and Laptop PC at testing site.

The system includes four 4-channel signal-processing modules, allowing data from up to 16 sensors or other measuring devices to be monitored, processed and saved concurrently. The data received from these modules is stored on a CompactFlash (CF) memory card capable of being removed to get the data directly if the need arises or is desired. The system is powered from an external source of either AC or DC power which enters the system through a surge protector and is in turn connected to the Circuit Breaker, allowing direct control of the entire system's power and an additional line of protection from electric surges.

Various connection ports are located on the system for different types of communication with the exterior devices. Other than the power input, network or PC connections and the sensor wires can also pass through the enclosure while maintaining a total seal and connect to the inputs on the 4-Channel boards. On the right side of the enclosure, partially seen in Figure 3-3 a port allows the system's access to a communication antenna connected to a PC modem found within the case. It is through this device that remote connections can be made if alterations are needed while the user is off site, and more importantly the data can be sent from the on-site location to a FTP website that can be accessed separately through a standard network connection.

The AE sensors recommended and supplied with the system are described as piezoelectric transducers, which are known for being highly sensitive to acoustic waves while remaining relatively cheap to create and maintain. In order to make sure that the acoustic waves are able to pass from the object to the sensor there must be a suitable substance between the sensor and the structure to maximize surface contact and wave transfer. This is usually done by use of an epoxy adhesive or grease on the material and sensor while being held in place with clamps. However, due to the size and shape of the structure in this project clamping would prove to be difficult, and an epoxy adhesive may damage the sensors when it comes time to relocate them on the structure. For these reasons a silicone caulking was used to create a firm connection between surfaces. This material is also able to be removed rather easily when it comes time to move the sensors themselves, without any recorded damage to the devices.

Software

The software designed by PAC is able to perform a variety of operations in both a live-action and post-processor conditions. However, the first step in setting up the unit's software is the same in both cases. In order to properly use the system the software needs to be configured to how the user wants it to function and what the parameters are needed in its use. This can be done simply by accessing the CF memory card from the system by connecting it directly to a personal computer. Eventually, the final part of the overall project will have the system use a wireless modem and connect to an FTP site at Kansas State University, but for the laboratory analyses being performed here the system is configured to allow a laptop computer with the proper software installed to communicate with the system through Ethernet ports.

In order to accomplish this, the system will be configured to work on a Local Area Network and be given a static IP address. After initial setup the card will be able to be accessed through an Ethernet cable and the use of a File Transfer Protocol (FTP) connection. At this point the system is ready to communicate with a separate PC by Ethernet connection or simply save all incoming sensor reading to the Storage Card for future use.

Communicating with the system

The first piece of programming is called ‘SH-II Client,’ which has been created by PAC specifically to communicate with the SH-II system after a hard-line, dial-up or wireless connection has been established. After the installation is complete there are multiple ways to make a connection, in this experiment the best way would be to use an Ethernet cable due to the proximity of the computer and system.

From here thresholds can be applied to all the sensors so that if there is a hit that occurs outside this filter it can be neglected immediately and not subjected to being analyzed on a sensor by sensor basis, saving time. Another ability of this program is a real-time Line Display of the sensors’ recognized and recorded events. In the future stages of the project, configuration of the system to upload files to an FTP site for data collection will be used in order to further use the remote capabilities.

Accessing and using the data

The data being stored on the flash card can be accessed by either direct or remote methods. Direct is the easiest to perform, where the memory card is removed from the system and inserted into a card reader for access. The remote access options allow the memory to be acquired by the user without stopping the system from collecting data. For the current stage of the project the information can be collected using a remote method. The user connects to the system by use of an Ethernet cable and opening a FTP site window. Using an IP address and administrator password setup earlier for the system, the flash card can be accessed directly through this process.

Upon collection of these files the ‘AEwin for Sensor Highway E1.00’ program, also designed by PAC, is used to manipulate the data into a usable form in any of several user-designed graphs. The primary functions of this program are to replay the data as if it was being collected live, creating useful charts in both 2D and 3D formats, combine separate files, convert the system's DAT file into a text file, allowing it to be uploaded and used in spreadsheet programs like Excel. This was used extensively to compare the initial data to the loads being applied to the structure at the time. With this option, the load applied and resulting acoustic data being recorded can be examined quite easily with or without filters being applied to the file if needed.

FRP construction and test setup

Three FRP bridge decks were built by Kansas Structural Composites, Inc., designated Panel-A, Panel-B and Panel-C. Each is comprised of a mostly hollow 74" long by 102" wide by 6" high structure made of glass fiber-epoxy material designed by the Kansas State team after stage one activities were completed. This design consists of three layers of plates laid up to create a sinusoidal wave and stacked upon one another with a flat layer of fiber between them. The structure was then wrapped in chopped-strand mat and the epoxy resin is allowed to harden, the resulting plates have a ridged cross section but are capable of tolerating applied bending forces. Throughout the tests discussed Panel-A was monitored at all times to some degree, while Panel-B was monitored only during instances where interaction between two panels was necessary. Panel-C was not used in this research at all and was held in reserve in case massive failure occurred in Panel-A or Panel-B. Panel-A can be seen in Figure 3-4.

Figure 3-4 Panel-A on testing platform.

The overall structure of the panels was designed to allow bending forces to exist without damaging it to failure under regular loading cycles. To help create added strength to the bridge structure, when used in series the decks will be interlaced with one another by use of tongue-and-groove connections on either end of the structure as shown in Figure 3-5 below.

Figure 3-5 Close-up of Lip-and-groove connection between two panels

During the analysis phase of this project each panel is supported on four steel I-beams spaced with regards to the ends of the panels, with one located at roughly 4” and 28” from either end. For a better understanding, a depiction of this can be seen below as Figure 3-6. These beams are held in an elevated position by each end allowing vertical movement of the structure, and the bending from applied forces, to occur.

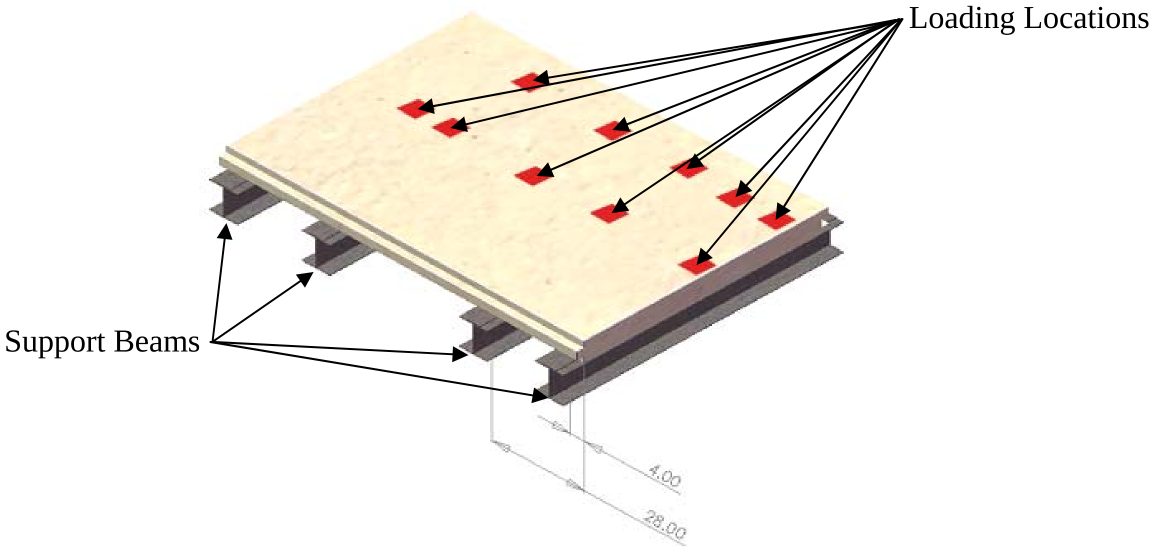

Figure 3-6 Bridge Deck and Support Beam Relation.

The bending force is generated by a hydraulic cylinder statically suspended over the structure, capable of applying forces anywhere on top of the panels. These forces can be in excess of 35 kips and applied in a way that allows for distribution to be over an area approximately the size of an automobile tire. This distribution is achieved by use of a specially designed “boot” on the end of the piston consisting of a steel plate and rubber-foam matting. This setup is similar to the one used in earlier analyses, except the forces exerted in this analysis are less than half of those used in the first stage. This is in part due to the analysis not requiring failure to occur, but just to examine how the data and sensors can be used to determine a source location. In addition, the first stage used a method that created uniform bending, where this stage uses a more specific loading location, allowing for the acoustic data source to be approximated easily; the most likely source will come from the point at which the plate is being exerted onto the panel, giving more accurate results if the plate is smaller. The items used to produce the direct force can be seen in Figure 3-7 on the next page.

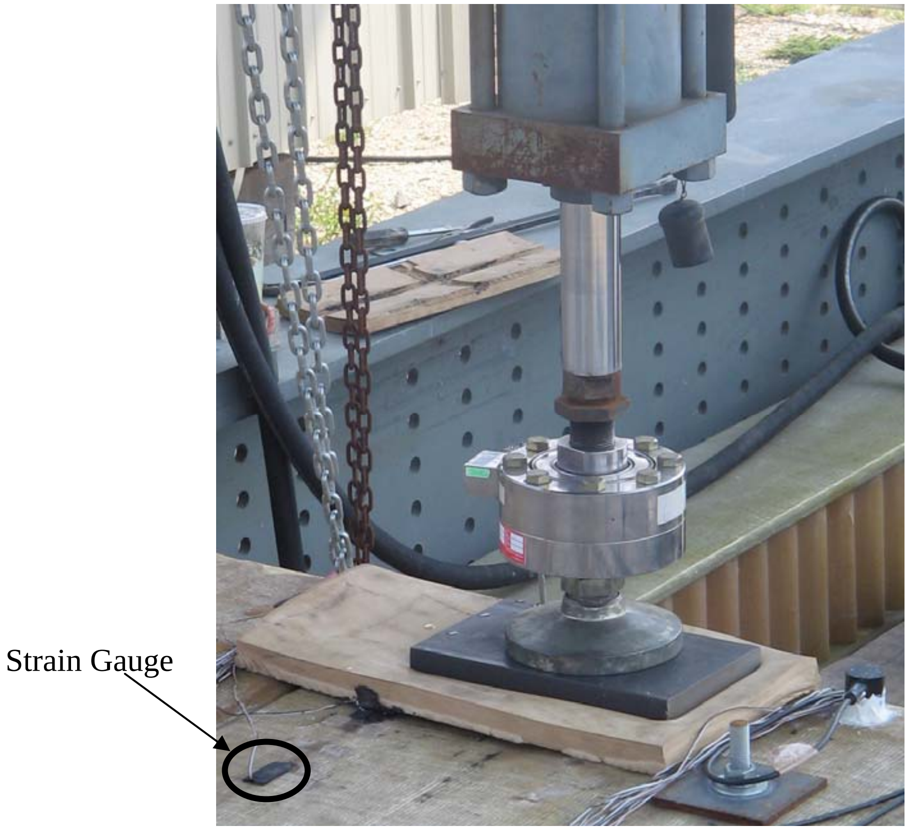

Figure 3-7 Pneumatic cylinder and distribution boot.

For the tests in this project the same procedure was applied in each case with the only physical changes being where the application of the force would be and the layout of the AE sensors. These changes in sensor location occur in response to the acoustic property being examined at the time as well as where the applied force is in the series of tests. The force location will be carried out at predetermined locations corresponding to placements between or over where the beam supports are under the panels.

During this stage there will also be another set of analyses conducted by Dave Meggers, who hopes to determine how the beam deflection, stresses and strains are related to each other by use of the data from the hydraulic cylinder, linear deflection and strain gauges. Some of these strain gauges can be seen in Figure 3-7, in the bottom left corner.

Thresholds

One concern of using this monitoring method is that the amount of data collected could create files so large they would become a problem when it comes time to transfer them over the modem later. In order to decrease these file sizes the data was analyzed with a variety of thresholds being applied to remove background and noise readings that occur regardless of the loading status of the structure.

Initial tests were conducted to determine if the system worked and what thresholds could be applied to the system during this analysis to remove as much excess noise as possible and focus on useful data. When no threshold is applied the background noise consists of persistent sounds that come from environmental, such as wind and rain, and mechanical sources, such as traffic and construction. While many other sources also exist, the largest in this project are going to be the mechanical sources primarily made up of the traffic noise. In this stage the traffic noise cannot be simulated to any reasonable degree, therefore the focus will be placed more on any constant noise that occurs during the tests overall.

The initial test took place by placing the sensors on Panel-A in a set of two arrays with two sensors located at places of interest. Due to the damage on the corner sensor S1 was placed on the side of the panel four inches from the corner. The other separate sensor was placed near the joint edge two inches from the edge and 81 inches in the X-direction, as shown in Figure 3-8 on the next page. The other sensors in the arrays were located at X-direction placements of 1, 11, 21, and so on up to 101 inches; and 18 or 28 inches from the joint edge, with the exception of sensor S10, located at twenty-four inches. The force was applied between the first and second beams at ten inches from the joint edge. This arrangement placed the closest sensor at just under nine inches, with the next closest at 18 inches.

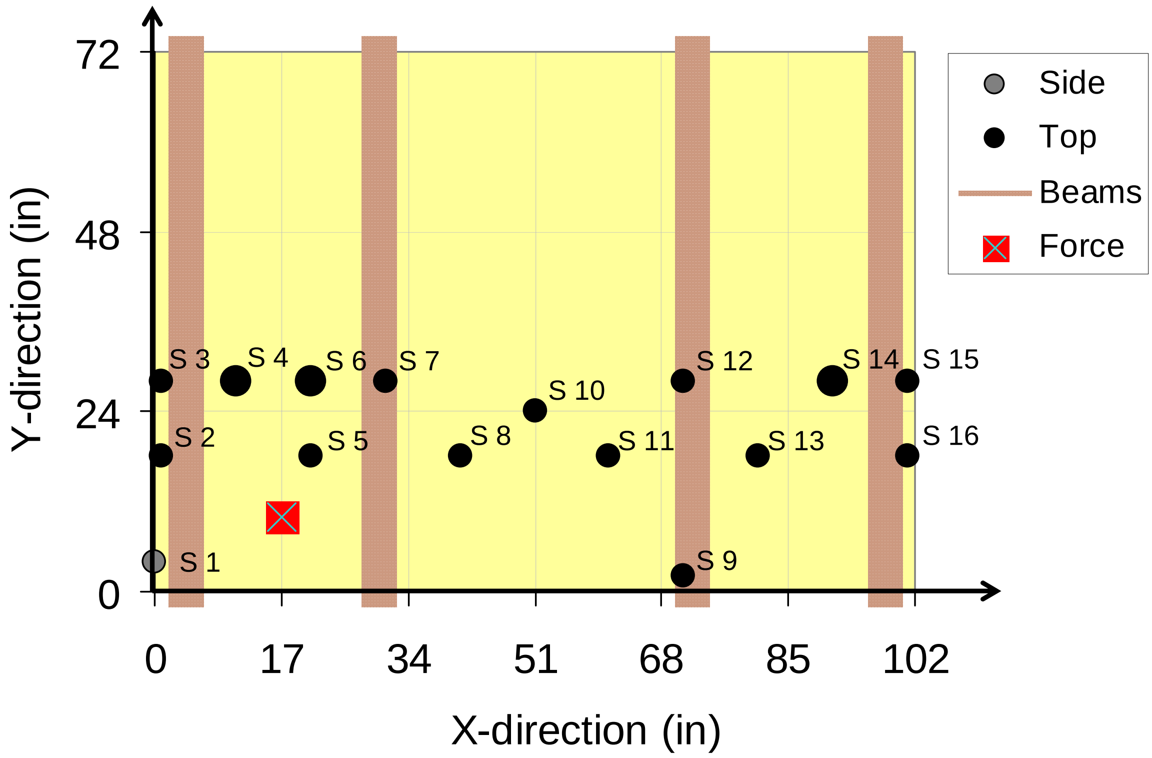

Figure 3-8 Threshold sensor arrangement

During the test a load was applied twice to the panel and recorded, acoustic data for both tests and the loading profile can be seen in Figure 3-9. The information gathered during the second application shows that there was a nearly-constant amplitude reading at about 35 dB, indicating a possible environmental or mechanical noise being detected. Indeed, when left to record data while no load was being applied the system reported hits were nearly constantly occurring between 20 and 40 dB. During subsequent testing a threshold of at least 35 dB would be applied to the system, and in later laboratory tests the threshold would be increased to 48 dB, to both remove noise and aide in keeping the file sizes small enough to be transferred easily.

A comparison of the data before and after the filter application can be seen in Figure 3-10 on the following page. The use of this single filter had a large effect on the file size as well as the data plots too. The original data file was 32 MB for a test lasting just under 1.5 hours. With the filter applied the data file can be reduced to only 2.42 MB, roughly 8.5% of the original file size. Also the characteristics of the data changes during increased loading occurrences are still present after the file cut down.

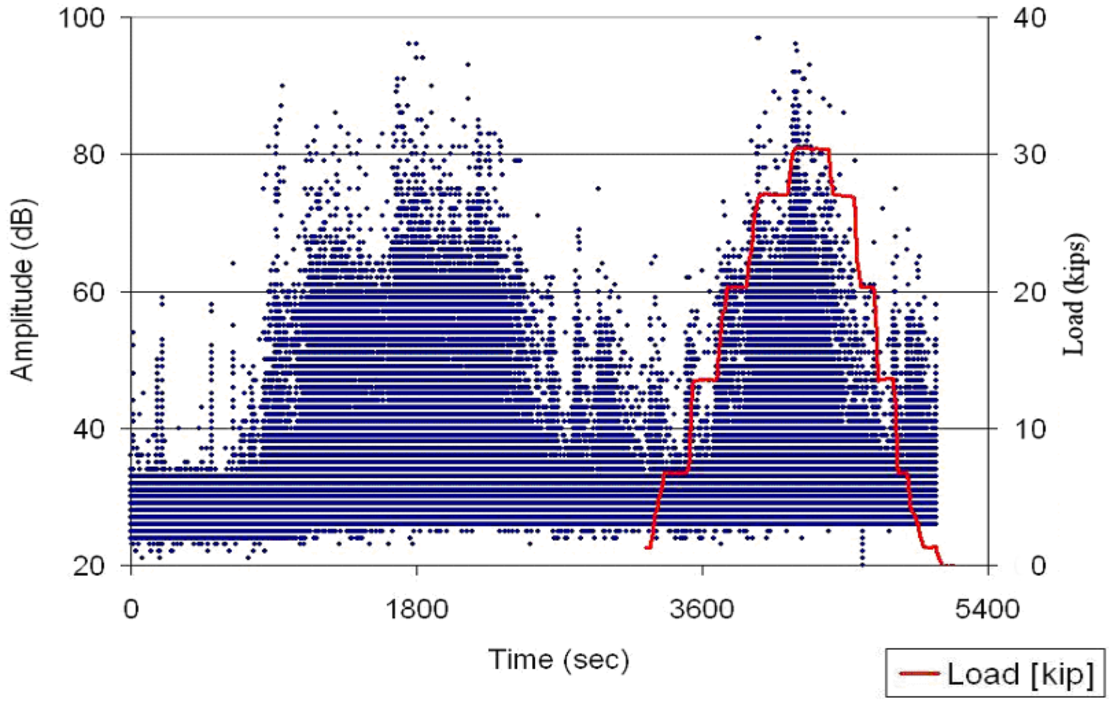

Figure 3-9 Initial analysis on an Amplitude versus Time scale.

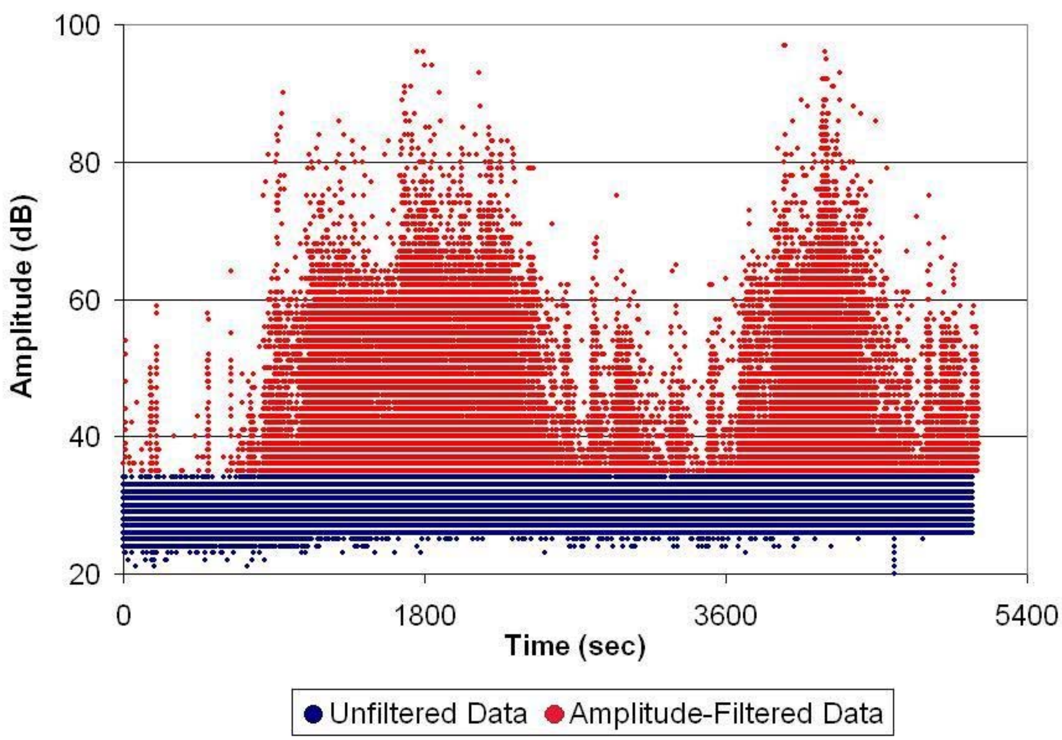

Figure 3-10 Thirty-five Decibel Amplitude Filter comparison

The next property that was looked at was the energy of the hits. These values can be seen in the figure below as blue and green dots. There seems to be a pattern of dots forming at about every ten counts and having several clusters at the 90 and 100 counts mark. If a 60 count threshold is applied to the data already setup with the amplitude threshold the green dots in the figure are the remaining points.

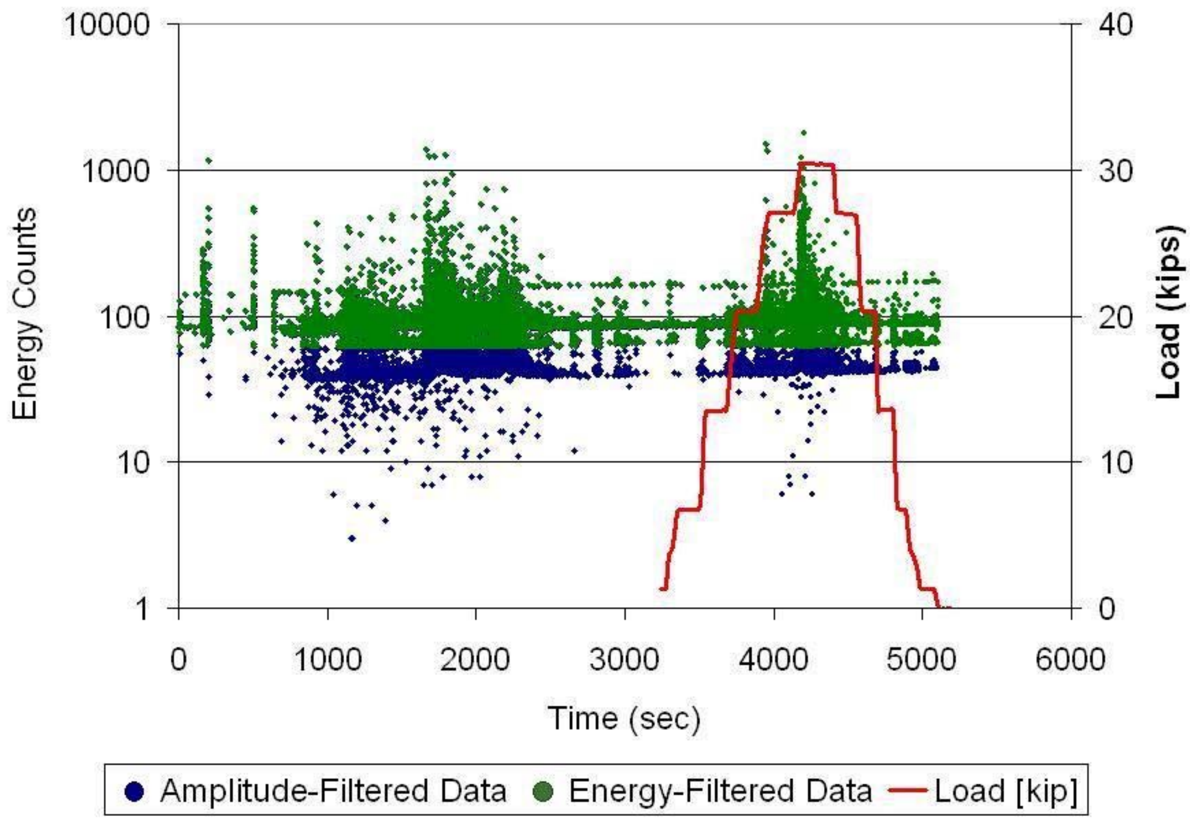

Figure 3-11 Energy comparison of 35 dB Amplitude and 60 Energy Count Filter

With this new threshold the data file actually decreases another 13.6% to 2.09 MB, making it so the data transfer later on could go even more quickly. At this time the original, unfiltered data was revisited and had only the 60-Energy Filter applied, with a resulting file size of 23.5 MB. This is a 26.5% decrease in size, and while not as great as the decrease from the amplitude filter, it is still significant.

In Figure 3-12 on the next page a comparison of the amplitude charts before and after the energy threshold is applied can be seen, and indicated that it has minor impacts on its appearance at this time.

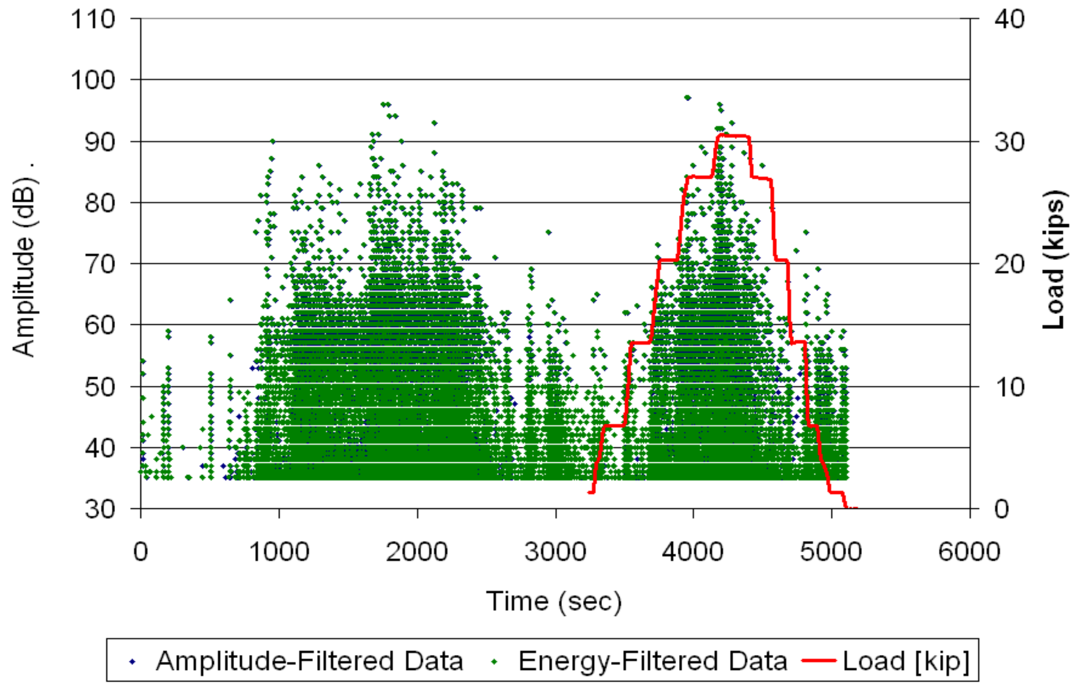

Figure 3-12 Amplitude comparison of 35 dB Amplitude and 60 Energy Count Filter

If the filter level is changed to 80 energy counts the chart is not altered much from the one above, but if an 85 count threshold is applied the chart starts to show significant change. As can be seen below, where hits at the beginning of the load in the analysis seem to be removed.

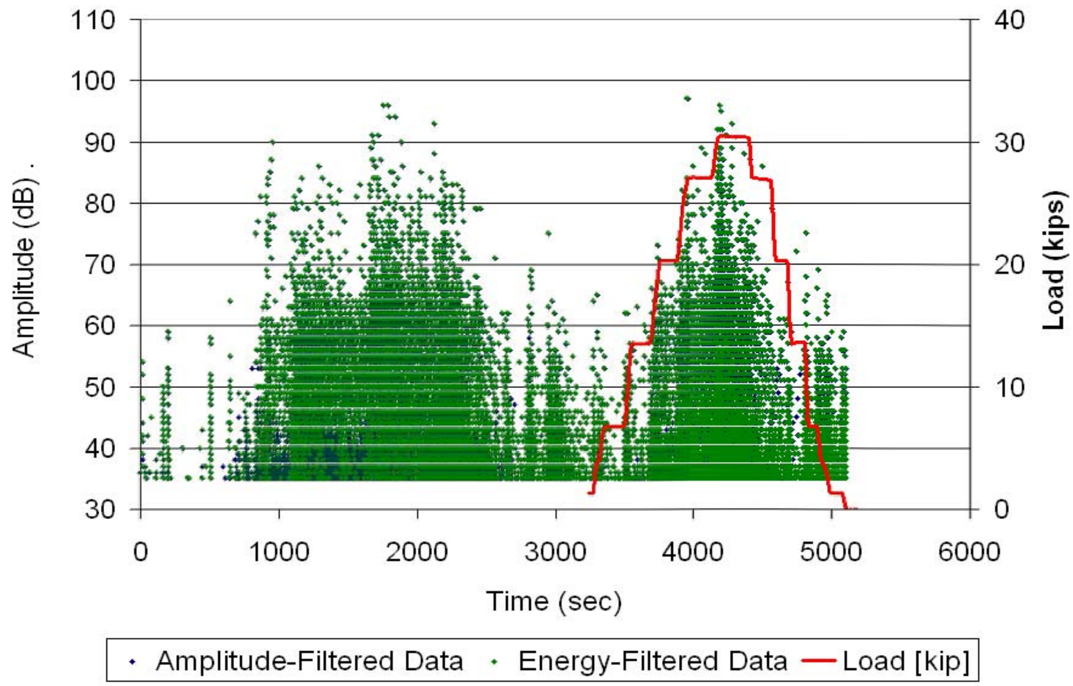

Figure 3-13 Amplitude comparison of 35 dB Amplitude and 85 Energy Count Filter

This is most likely a result of some sort of settling occurring in the panel, or small fractures forming and expanding during the first loading cycle, and breaking more in the second cycle.

A hit occurrence chart can be seen as the following figure. There are indeed a large number of points located below the 35dB mark on the chart, appearing between 10 and 100 times more often then the rest of the hit values. By applying the 60-Energy Filter the data decrease appears to be on the lower end of the remaining amplitude data points. There seems to be a small hump of data between the 35 and 48 dB values remaining, and a majority of the second filter takes the data out of that section only indicating high energy is related to high amplitude.

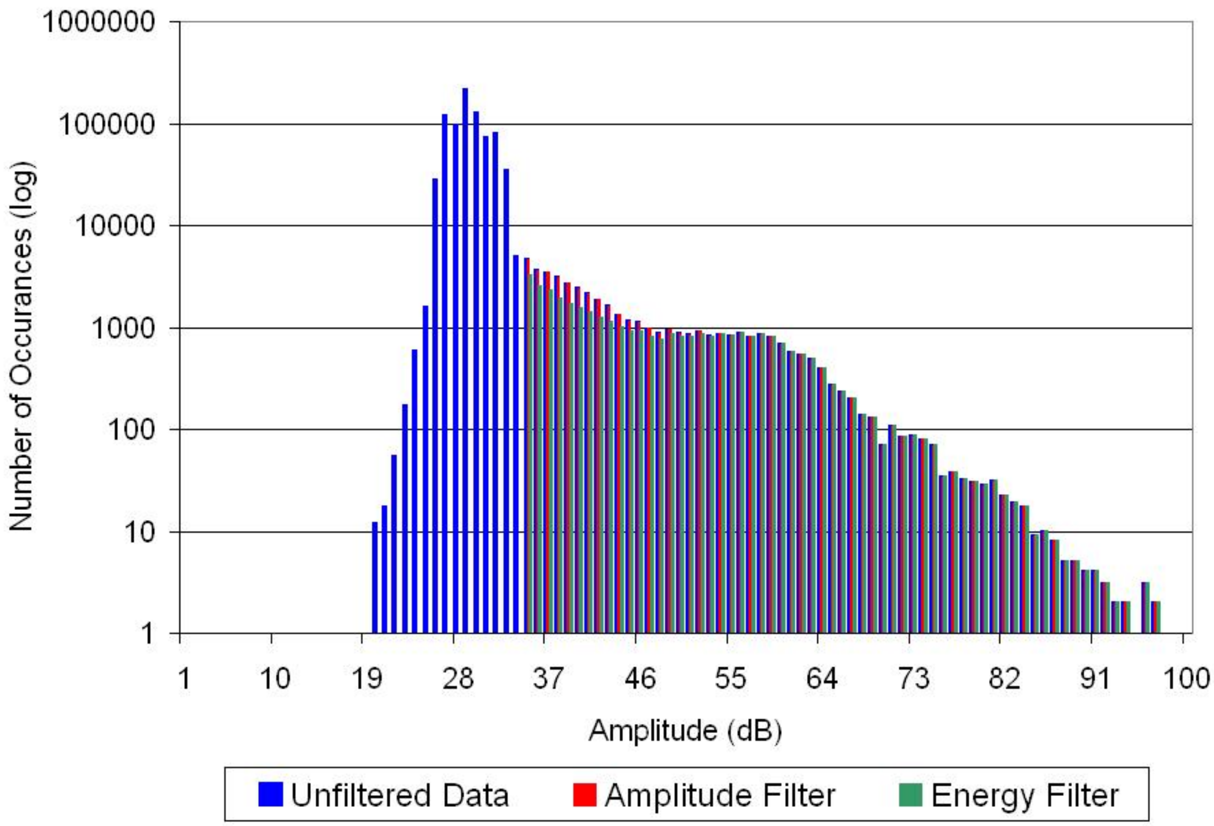

Figure 3-14 Change in Hit Number by applying 35-Amplitude and 60-Energy Filters.

During this stage of testing the file size is not important, as the data will not be transferred remotely, and therefore the thresholds used at this time will include an amplitude filter, as well filters for values below 1000 of signal strength. The data is not limited as much as in the filters presented for possible future use, but does remove data at lower Energy Counts.

3.3 Signal distribution in single FRP panels

The future bridge sensor layout will need to be built so that the limitation of a sensor does not become a limitation for the entire sensor network. To do this a series of tests were conducted to determine what manageable range the sensors have and how features in the panel affect the signal's ability to be recorded.

Basic analysis of single panel load response

There were two tests completed over each of the first three beams, as well as one between each of the same beams. The tests themselves consisted of an increasing step load being applied over time. The first load would start at around one-thousand pounds and increase incrementally to the maximum load being targeted. These increases in load would occur over a few seconds, at which point a load would be held for at least two minutes, at which point then the next load increase would occur. Upon reaching the maximum desired load, it would decrease in a similar fashion to the increase in load until reaching a load free state.

Before continuing it should be noted that while the original intent was to take the load to a maximum value of around 22.5 kips, there was a calibration error in the load cell used by the facility performing the loading tests. This was not discovered until after a majority of the tests were performed, and resulted in an increase in the load of about thirty-six percent. The analyses presented here have reflected the appropriate change in the load values, but as stated, it was not the intent to use this much load during the earlier stages of this project.

For the first examination the data will be displayed as functions of time with the applied loads overlaid on the graph. From this we can determine if there is a relation between the AE values and an applied load. This is the first step in determining if AE monitoring can be used as an acceptable form of determining structural damage to the panel. While the panel is not actually experiencing overall failure the increase in stress should cause small fiber and matrix breaks, as well as general mechanical noises.

This test will have all the sensors on Panel-A in the same configuration as was used in the initial threshold test as shown in Figure 3-8, in a set of two arrays with two sensors located at places of interest. The forces were applied at various locations on or between the support beams in the tests, but the following data comes from the force application between beams 1 and 2 as was used for the threshold.

From Figure 3-15 we can see that there is indeed an increase in the AE activity whenever the load applied increases and response seems to be in some way proportional. This means that when the load increases the amount of AE data created seems to increase in both the magnitude and amount of hits.

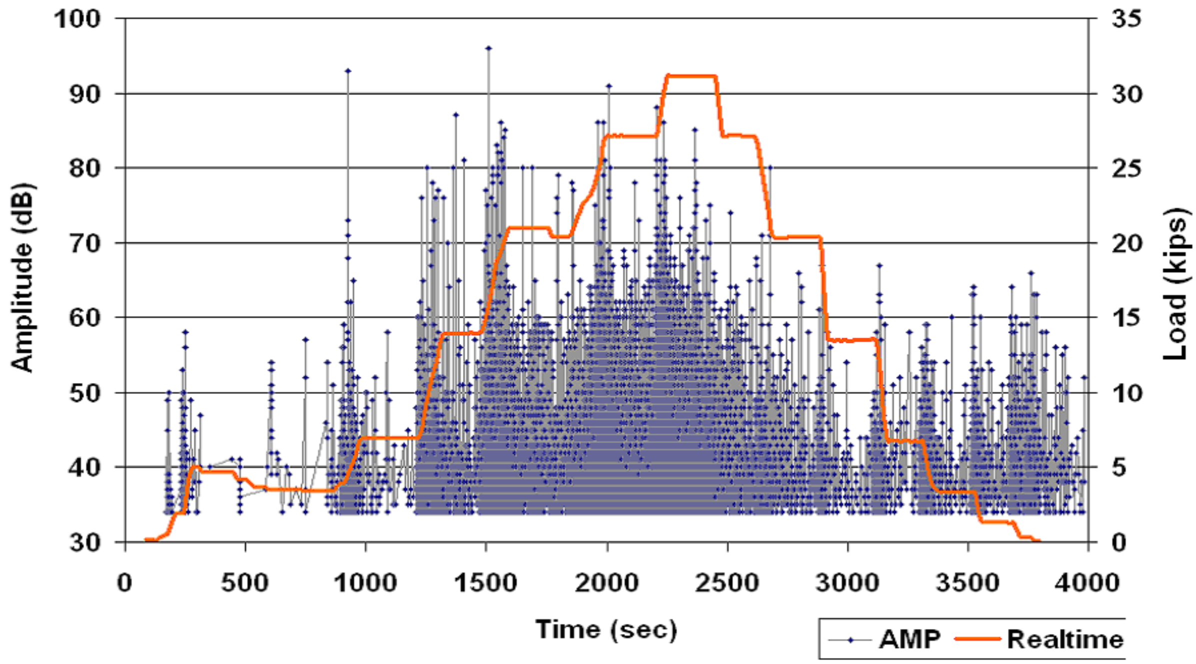

Figure 3-15 Initial test, Amplitude with Force overlay.

It is also reasonable and shown in the figure that when a larger load is obtained the AE activity occurs without a significant drop. This is most likely due to continuous fiber breakage and resin cracking; as the load is applied the initial, weaker, fibers within the structure will break along with weak spots in the resin. This breaking of materials creates an increase in the amount of stress being experienced in the remaining local structure, these pieces then fail as their ultimate stress values are surpassed, creating more stress for the material, and the cycle continues. This scenario can also be seen in the values of energy and signal strength charts included in Figure 3-16 and Figure 3-17 on the next page. These properties experience a greater amount of variation in their values, and need to be displayed on a logarithmic scale in order to get a greater understanding of the information.

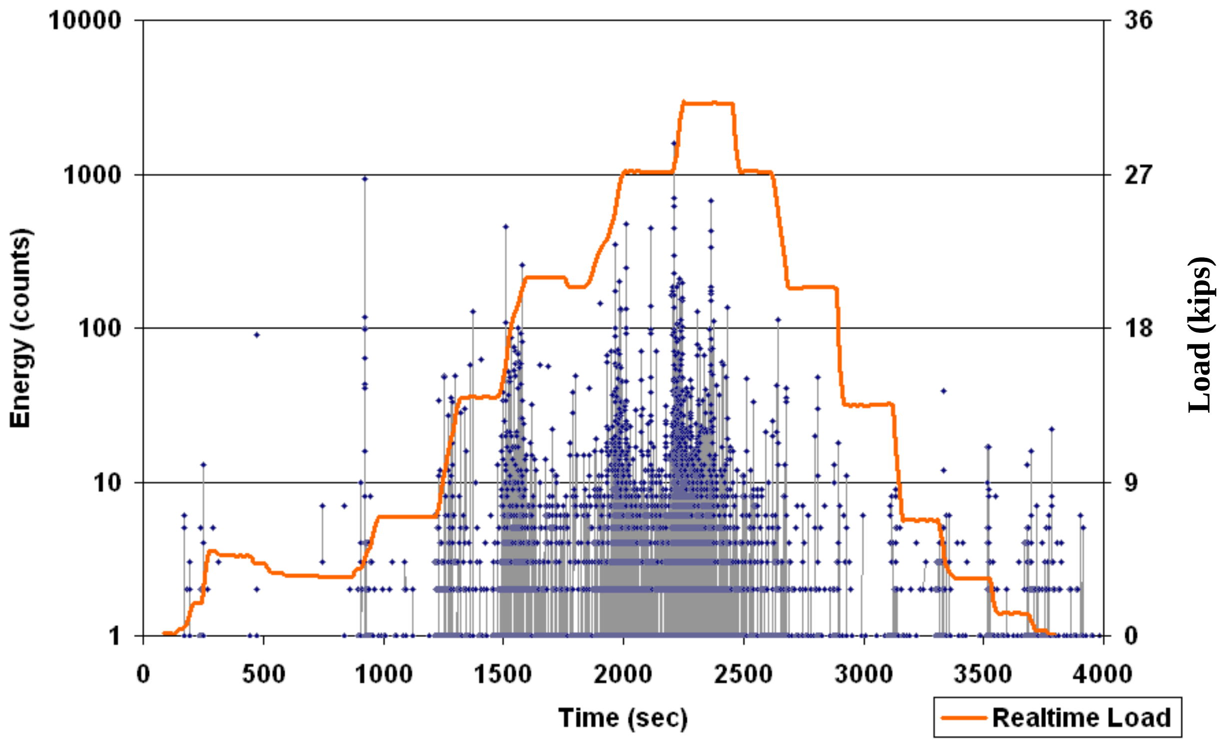

Figure 3-16 Energy Response with Load overlay.

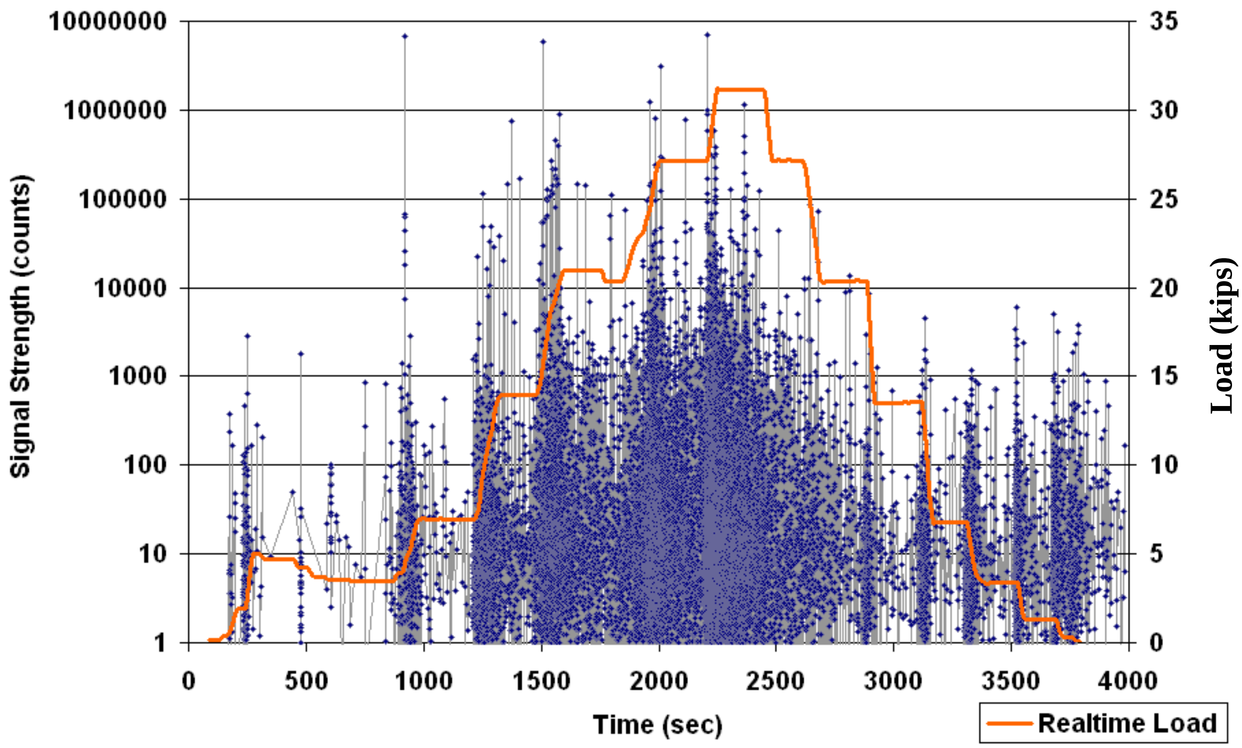

Figure 3-17 Signal Strength Response with Load overlay.

Single panel acoustic dispersion analysis

The sensors were arranged in two arrays along the top of Panel-A, as with the earlier tests, but three sensors have now been moved to the underside of the panel, as shown in Figure 3-18. By doing this an accurate assessment of what the degradation of the acoustic properties is in relation to increasing distance from the source can be generated effectively.

As earlier each test had a force applied on and between each beam, but the data from the beam 1 and 2 midpoint will be discussed at this point.

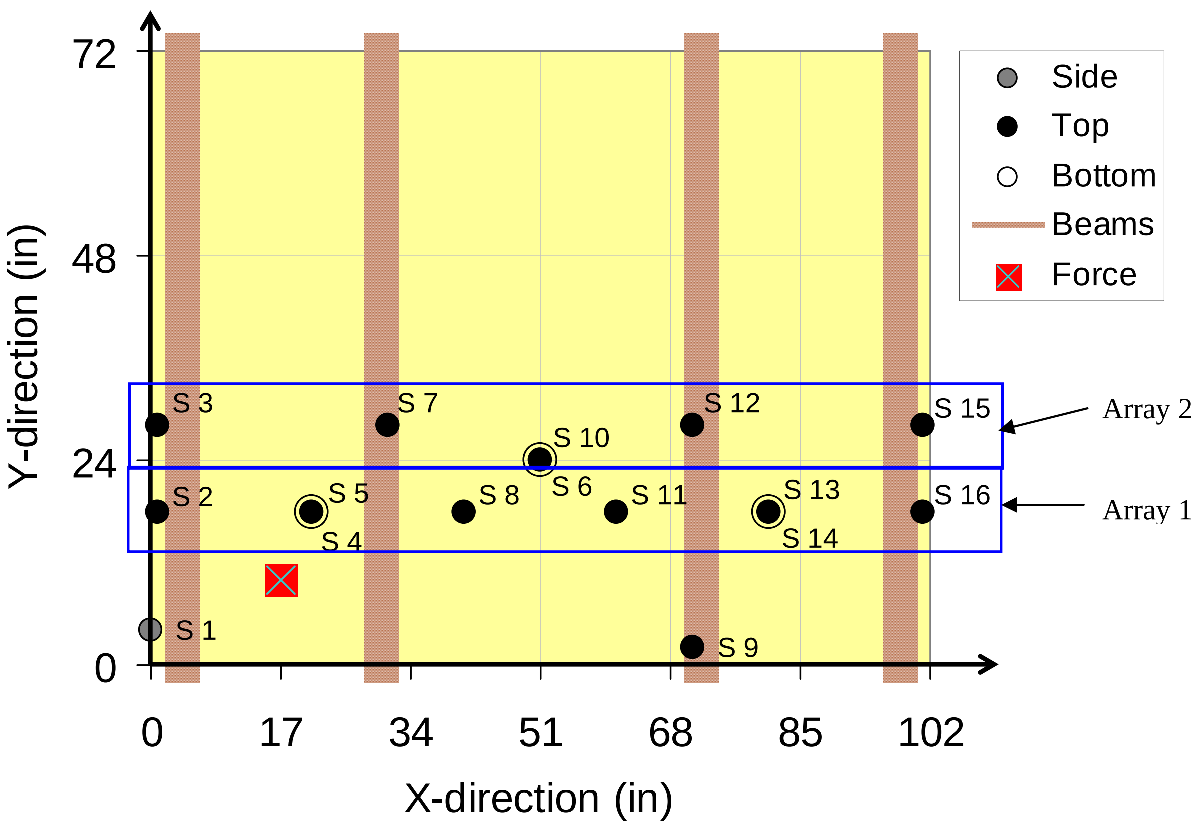

Figure 3-18 Signal Dispersion sensor arrangement.

In this case three tests were conducted in which the force was applied in the same location, and in the same manner as in earlier exams by stepping up to a force of about 30 kips and stepping back down again. This will present the opportunity to see if the results of a test can be repeated and still get approximately the same data, or if there is any pattern to the results at all. After the tests were concluded the results were graphed in terms of where the sensor was located horizontally with the panel's width. The force was not located in-between or on either line of sensors, but was located at ten inches from the joint edge, making it placed at about 18 inches from the array made up of sensors S1, S5, S8, S11, S13, and S16. This set of sensors will be designated Array 1 to make it simpler to discuss in the rest of the paper; the second set will be designated Array 2. This set is made up of S3, S7, S10, S12 and S15. The S10 was included in this array even though it is actually located between the two arrays to place set of points between the S8 and S11 points in later graphs.

The first analysis was conducted to determine what effect the loading amount has on the properties of each sensor. In Figure 3-19 below, it can be seen that while the force value increases the magnitude of the energy does as well in each of the sensors. As would be expected the sensors near the loading zone show an increased magnitude in relation to the other sensors, creating a hump like shape to occur around the sensor located at the 21 inch mark, S5.

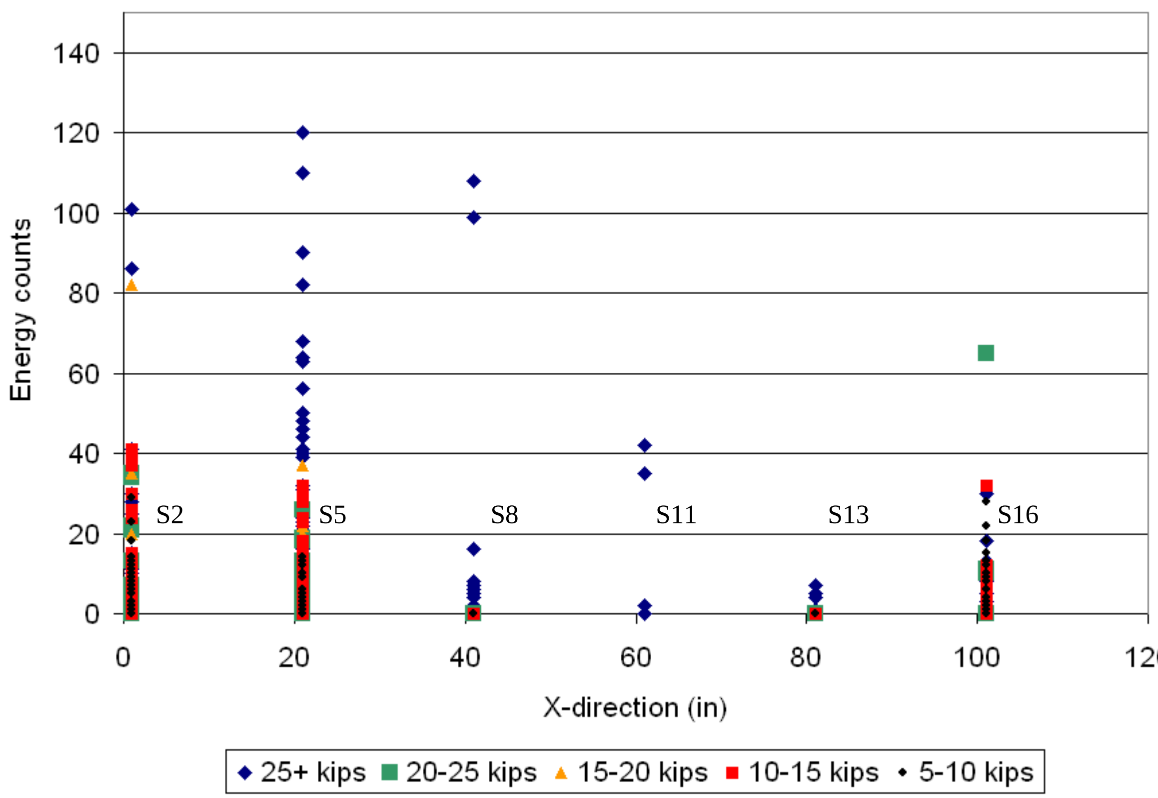

Figure 3-19 Energy values across sensor array 1.

This occurrence was also found to happen in regards to the signal strength, amplitude, and the general number of hits as well. The values were found to focus in on one section of the array quite well when examinations were conducted above the 25 kips mark, which is most likely due to the high number of hits, as shown in Figure 3-20, that were detected during this period of heightened force application. If the values over 25 kips are removed from the chart, as in Figure

3-21, a pattern is still noticeable for the other four ranges, where initially a large number of hits occur when the force is lower and as increases begins to decrease significantly. After this initial drop-off the value increases for each higher range, and a defined hump occurs again. From these multiple charts a definite pattern of increased activity and magnitudes can be seen near where the force is being applied.

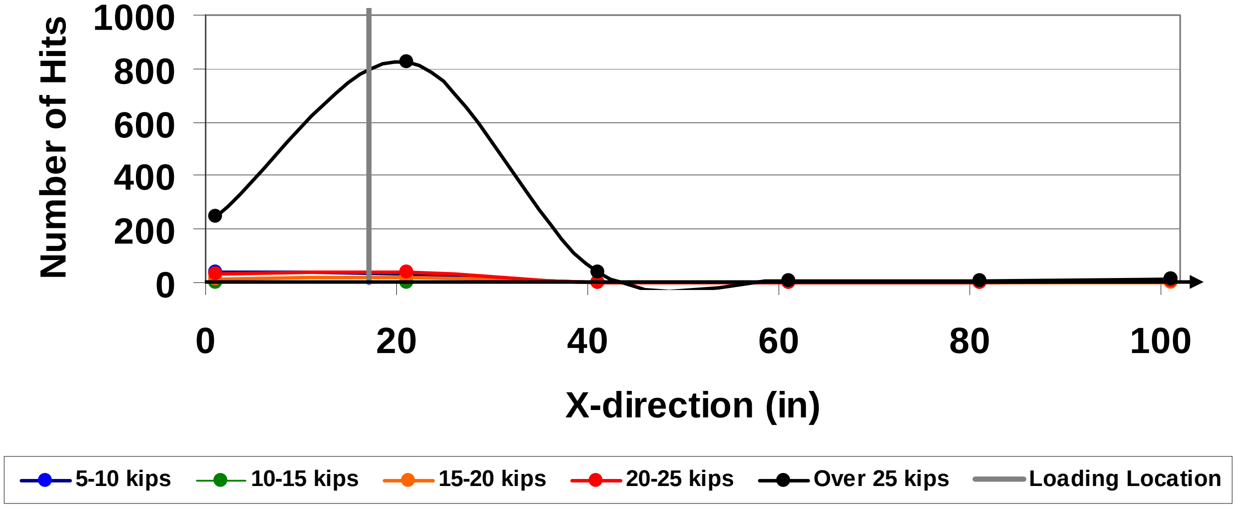

Figure 3-20 Number of Hits across sensor array 1.

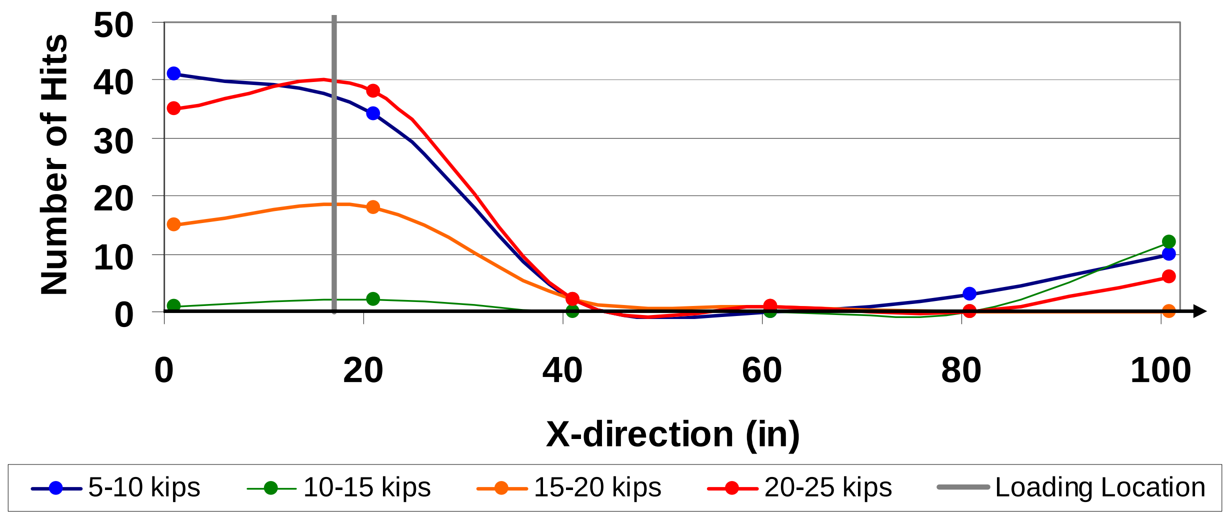

Figure 3-21 Number of Hits across sensor array 1; between 5 and 25 kips.

If the number of hits that each sensor detects is plotted, as in Figure 3-22 and Figure 3-23, the hits can be used to get an approximate location of the loading point, but in terms of the testing order, there doesn't seem to be a pattern when below 25 kips, but the values are still similar in terms of the magnitude. The pattern of decreasing in magnitude during each testing sequence does occur once the load is over 25 kips. In either case, each test still could be used to determine the general area of and further aide in locating where the source is closest to the sensor array.

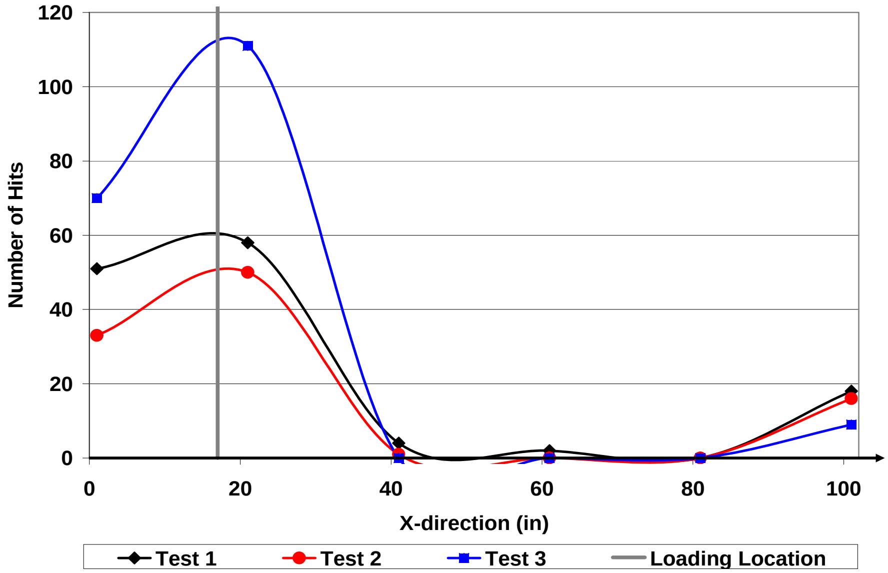

Figure 3-22 Number of Hits on sensor array 1; Over three tests, under 25kips.

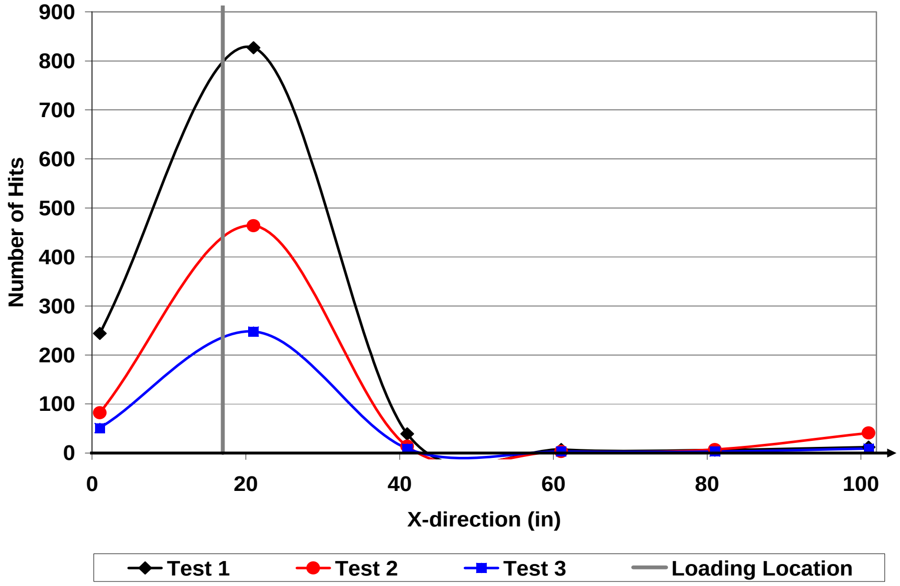

Figure 3-23 Number of Hits on sensor array 1; Over three tests, over 25kips.

In the following sets of figures the repeatability of the findings is explored further. In Figure 3-24 it is shown that during the three testing sessions the values were similar and show the same general trend to demonstrate that the source location is generally near sensor S5. However, another pattern can be detected as well, the decrease of overall values. While each test has values that are similar, they decrease after the first analysis when near the source. As can be seen from the figure, at a distance from the source the values decrease until reaching the sensor on the opposite edge of the panel, and do not follow any type of pattern in that the highest values come from the third test and the smallest is the second with the first being somewhere in the middle.

Sensors closer to the source have somewhat of a pattern in magnitudes. As the tests are performed the values decrease, meaning that after the first test it would take more force to obtain similar values of the previous test. As with the hit-figure on the last page, the occurrence most likely has to do with the panel cracking in places during the earlier tests that now have a lower stress from the same bending load being applied.

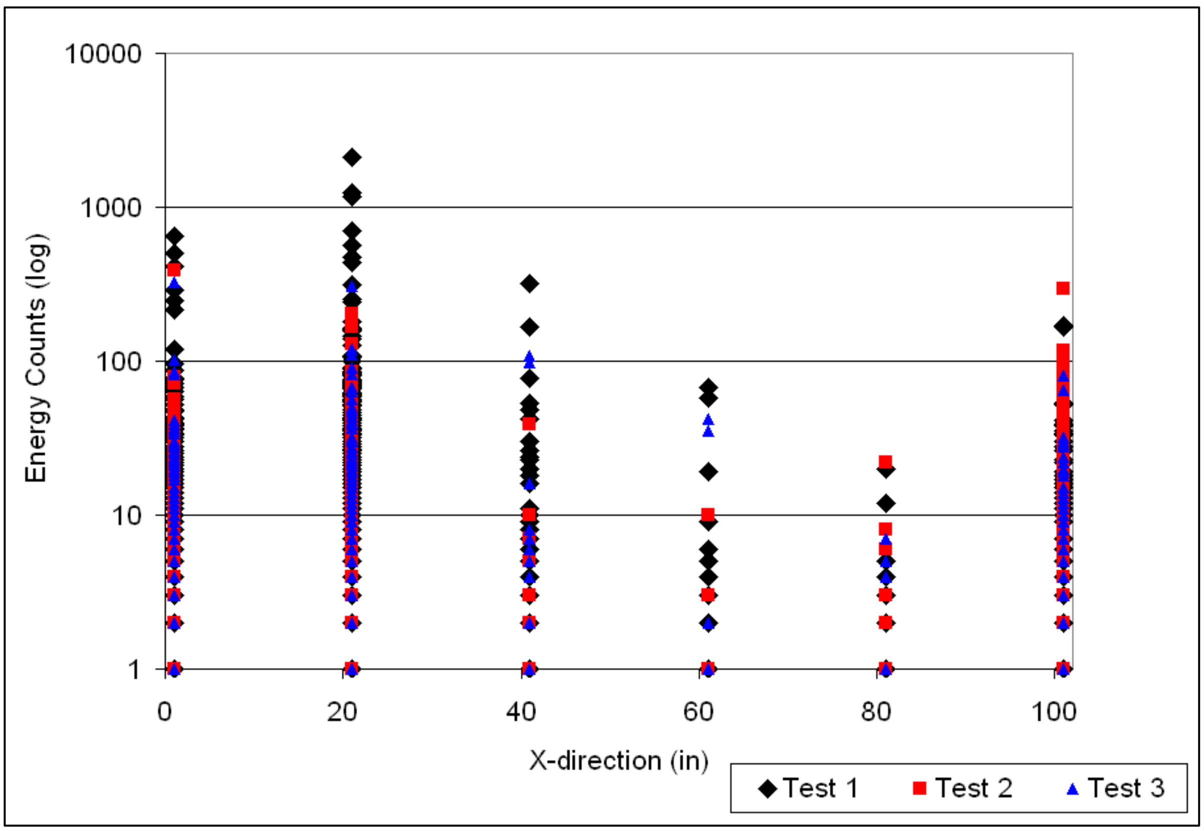

Figure 3-24 Absolute Energy values across sensor array 1; Over course of three tests.

The last part of this section will demonstrate the usefulness of having the two arrays present during the testing. If we were to look at the first array without any knowledge of where the source was located, at this point it would be most likely that it would be between beams 1 and 2, and closer to sensor S5 than to S2. And thus far the belief would be correct. But how would the source location be known in terms of which side of the array the source is on?

In order to solve this question, the second array can be employed quite easily, and effectively. When the second array is plotted with the first, as in Figure 3-25, a pattern emerges that shows that at distances farther from the source location there appears to be a steady increase similar to both arrays, shown with the green line below. The data from the sensors near the presumed source are more defined, and show that Array 1 has higher values than Array 2; therefore the source would either be between the arrays, yet closer to Array 1, or on the side that is closer to the joint edge. While not a full network, the simple use of two arrays has narrowed down the location of the source to a small section of the overall panel.

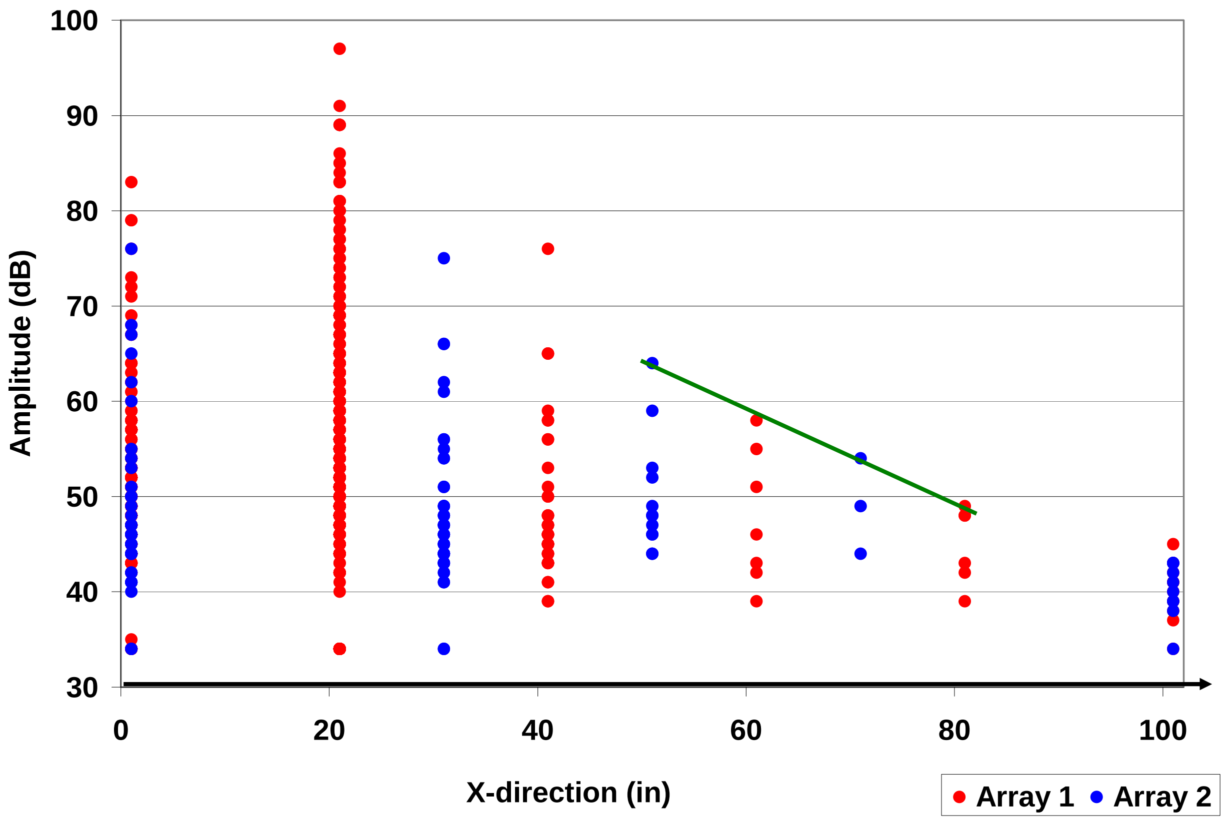

Figure 3-25 Amplitude values across sensor array 1 and 2.

A further analysis of this technique shows that the number of hits recorded by each array is significantly different with the first having a larger amount overall.

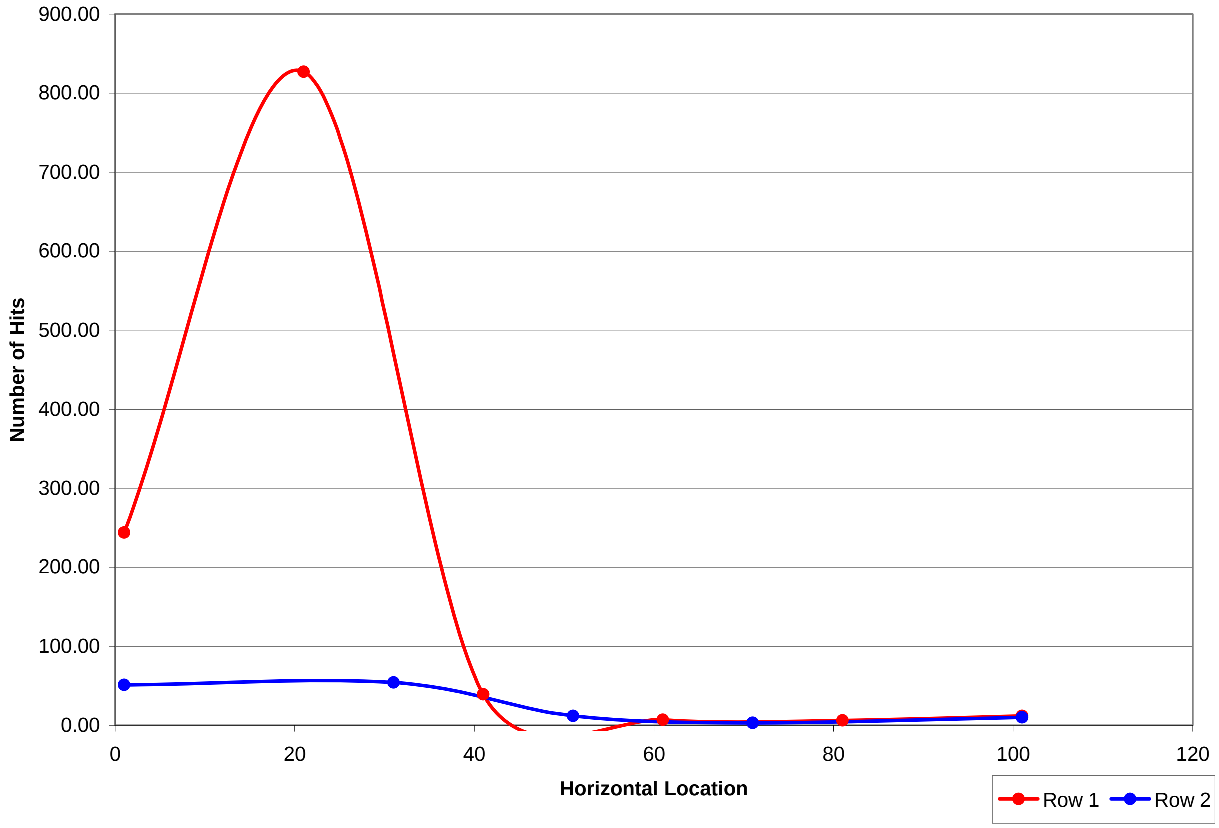

Figure 3-26 Number of Hits across sensor array 1 and 2.

Another phenomenon that can be seen from several of the previous figures is that the number of hits seems to decrease dramatically at around the 30 inch location, which happens to be near where a support beam is located. This decrease seems to be mostly from the lower energy and strength events, resulting in 'small powered' fractures possibly going unnoticed across the beam. This means a set of arrays would need to be located between each beam if small energy events needed to be recorded.

3.4 Acoustic degradation analysis

By using the same data as in the last analysis, a pattern emerges in the values for energy when plotted with relation to the distance of the sensor from the load. A decrease in the general properties is noticeable as the sensors are placed away from the source of the acoustic signal. This follows the same basic principle that was discussed by use of the arrays, but in this case the average values for all the data at a point is used, rather than just the high load time-spans. This might show that if the average values for a network of graphs were plotted, the resulting chart might give the researcher a hint as to where further analysis should be conducted to determine if there is cause for concern.

The property that shows the greatest difference between distance points is that of the absolute energy as plotted in Figure 3-27, below. In this figure we can see the decrease in magnitude as the distances increase. In this case the best plot was found to be that of a 'Power Trend-line', not all that surprising as a great deal of acoustic properties have an inverted second-order relationship with regards to distance from the source. It seams in the case of AE in a FRP panel the relationship is no different, as that general trend exists here as well.

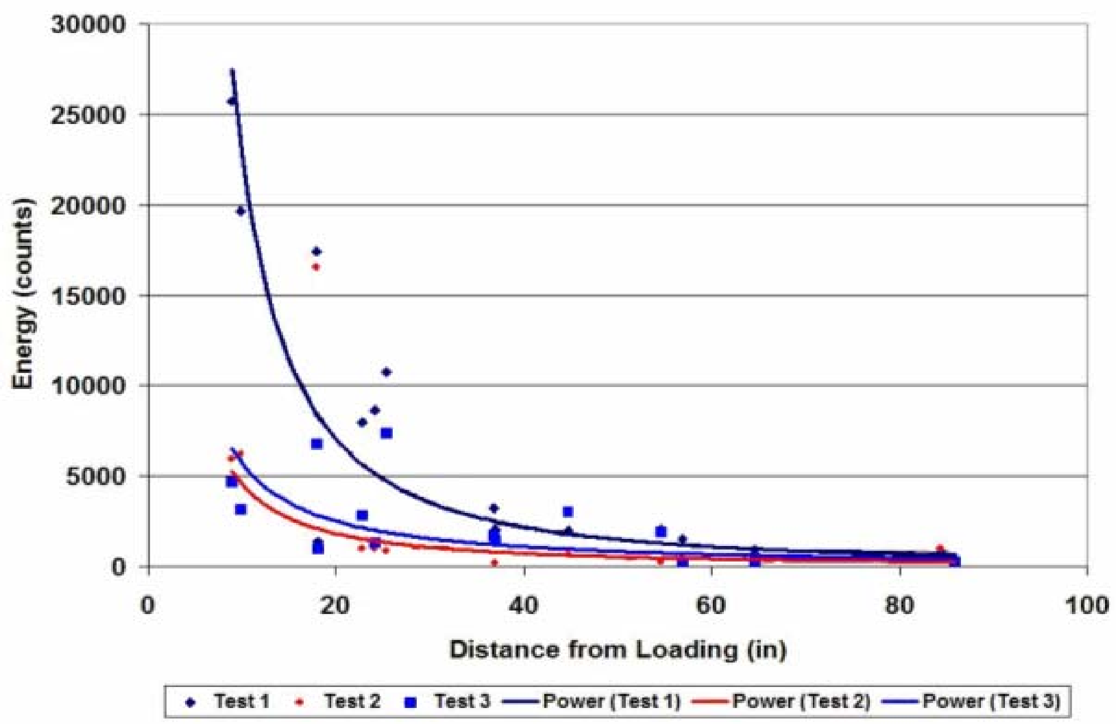

Figure 3-27 Average absolute energy plotted at various sensor distances.

The next property examined is that of the amplitude data. From the figure shown on the next page we can see that a similar trend is experienced as that in the energy plot on the last page.

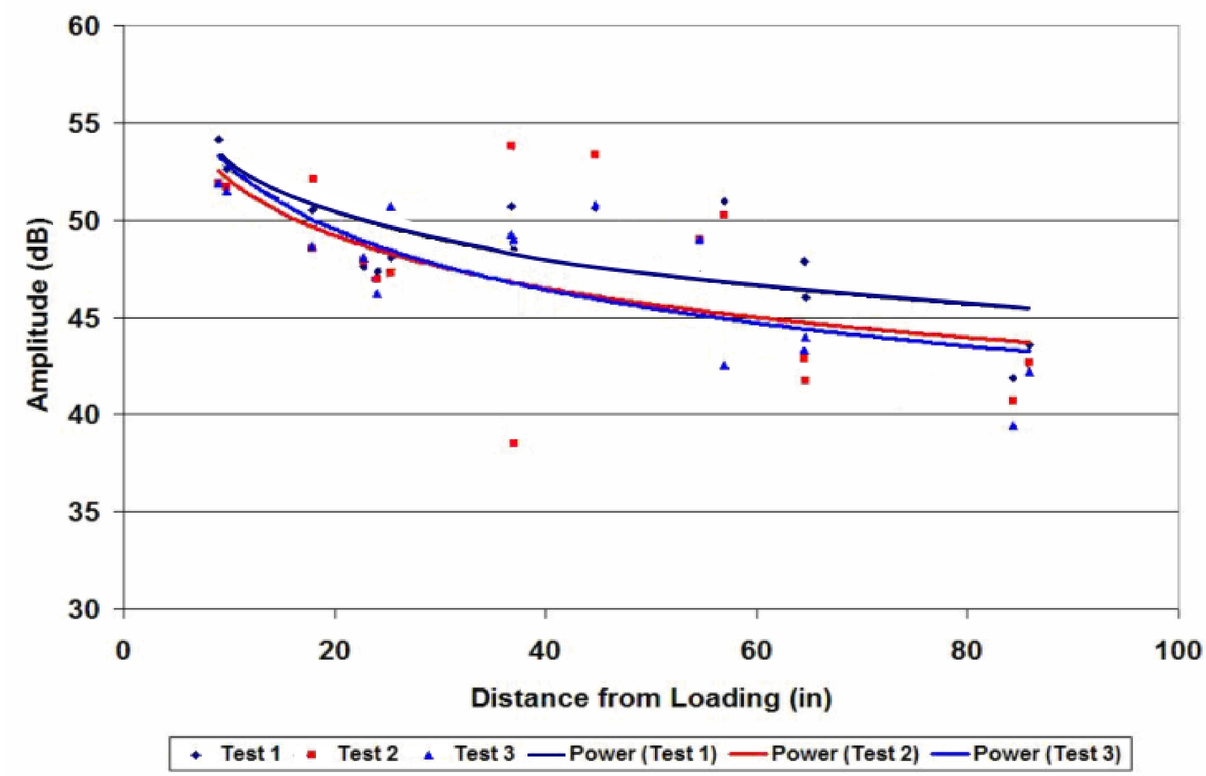

Figure 3-28 Amplitude plotted at various sensor distances.

In all of these property graphs the three tests plotted seem to show normalization to a linear relationship or practically none at all in regards to the distance after approximately thirty inches has been reached. This data strongly substantiates the determination earlier that sensors outside two feet were found to be much lower in both magnitude and amount of data recorded.

Given the information collected, a distance of approximately one to two feet should be observed when mounting the sensors on the actual bridge panels. This range would allow strong values to be recorded for the various signal properties when within the loading region, examination of the graphs, and the desire to have as large as possible area covered by the sensor net. In the preceding graphs the properties show a habit of following the trend-lines better up to two feet from the source and becoming erratic soon after this range has been surpassed. The interior limit was chosen due to large values being detected near the source, and the general idea that the sensors being too close together would be redundant and unnecessary.

The last analysis for sensor placement involved the use of the sensors on top and on bottom of the panels, as well as possible benefits of using one over the other. For this testing set the layout was changed once again to reflect the need to compare data taken on the panels' tops to that of the bottoms. This testing set has the force application occur directly to Panel-B, while

Panel-A records data from the transfer of the acoustic signal across the joint. The sensor layout designed and used for this analysis is shown below in Figure 3-29.

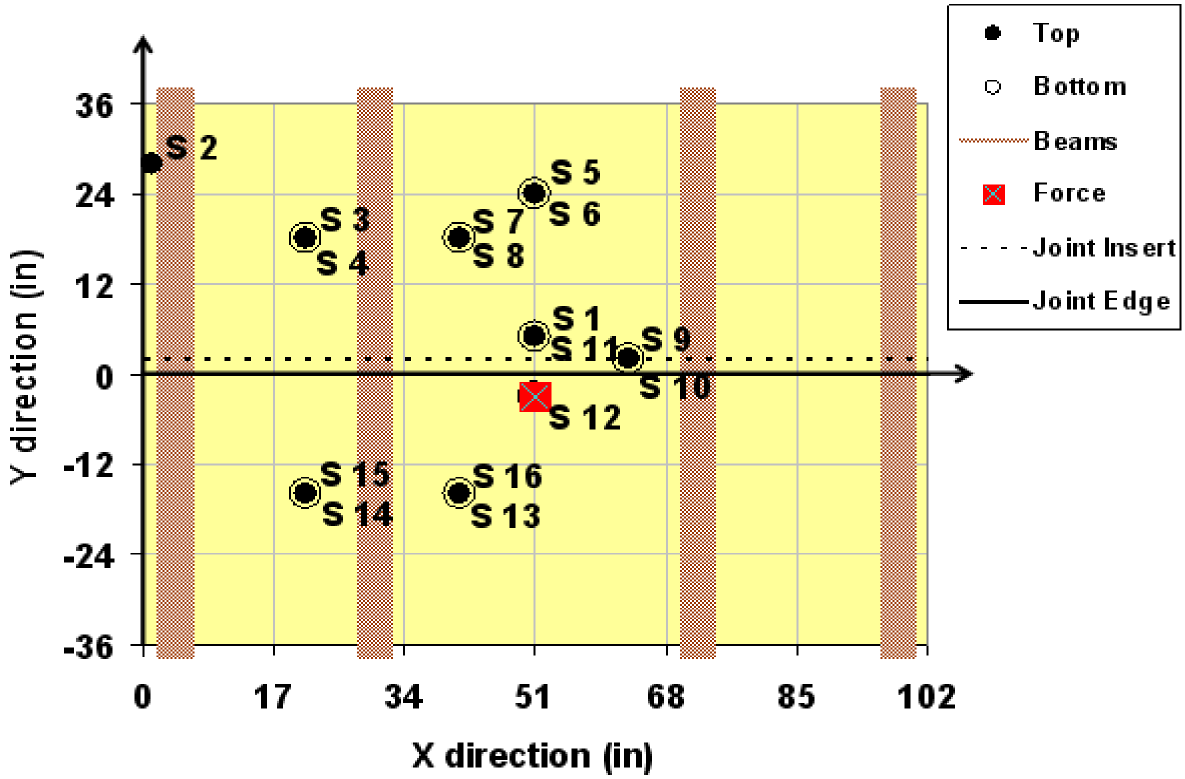

Figure 3-29 Degrading Signal sensor arrangement.

Upon graphing the data all of the sensors on top and within two feet of the force application location, situated over sensor S12, show a strong resemblance to their corresponding sensors located on the underside of the structure. The exception is sensor pair S13-S16, where sensor S13 detached partially from the panel before the silicone could harden and record a proper set of complete data. Of the sensors outside the two foot radius the S5-S6 pair did record data very similar to the S7-S8 sensor pair, located approximately four inches closer to the load, but all other sensor pairs recorded little data.

The closest sensor pair is S1-S11 and when plotted, as shown below, shows similar concentrations of data point peaks. The sensor located on the bottom of the panel, S11, has an increased number of data points and is most likely related to the interaction between the panel and support beams or the joint between panels. In this case the latter would be more likely.

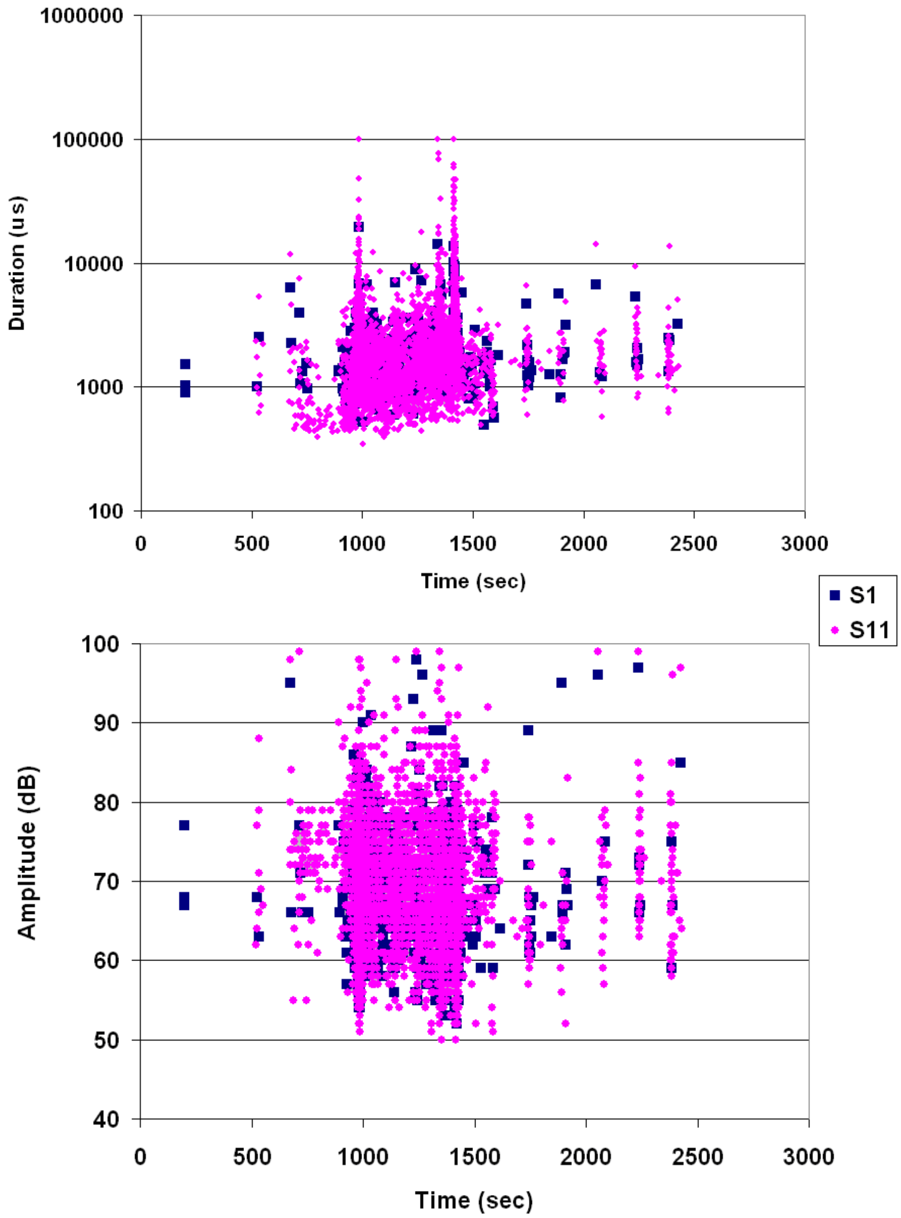

Figure 3-30 Duration and Amplitude comparison of sensors; S1 on top and S11 on bottom.

Indeed if the sensor pair S9-S10 is examined, a strong comparison can be made between the sets of data points. The individual sensor pairs can be seen on the next few pages, through page 47. From the findings in this section it seems that as long as the sensors are placed closer than two feet from each other and secured properly, it does not matter if the sensors are placed on the top or bottom of the structure overall.

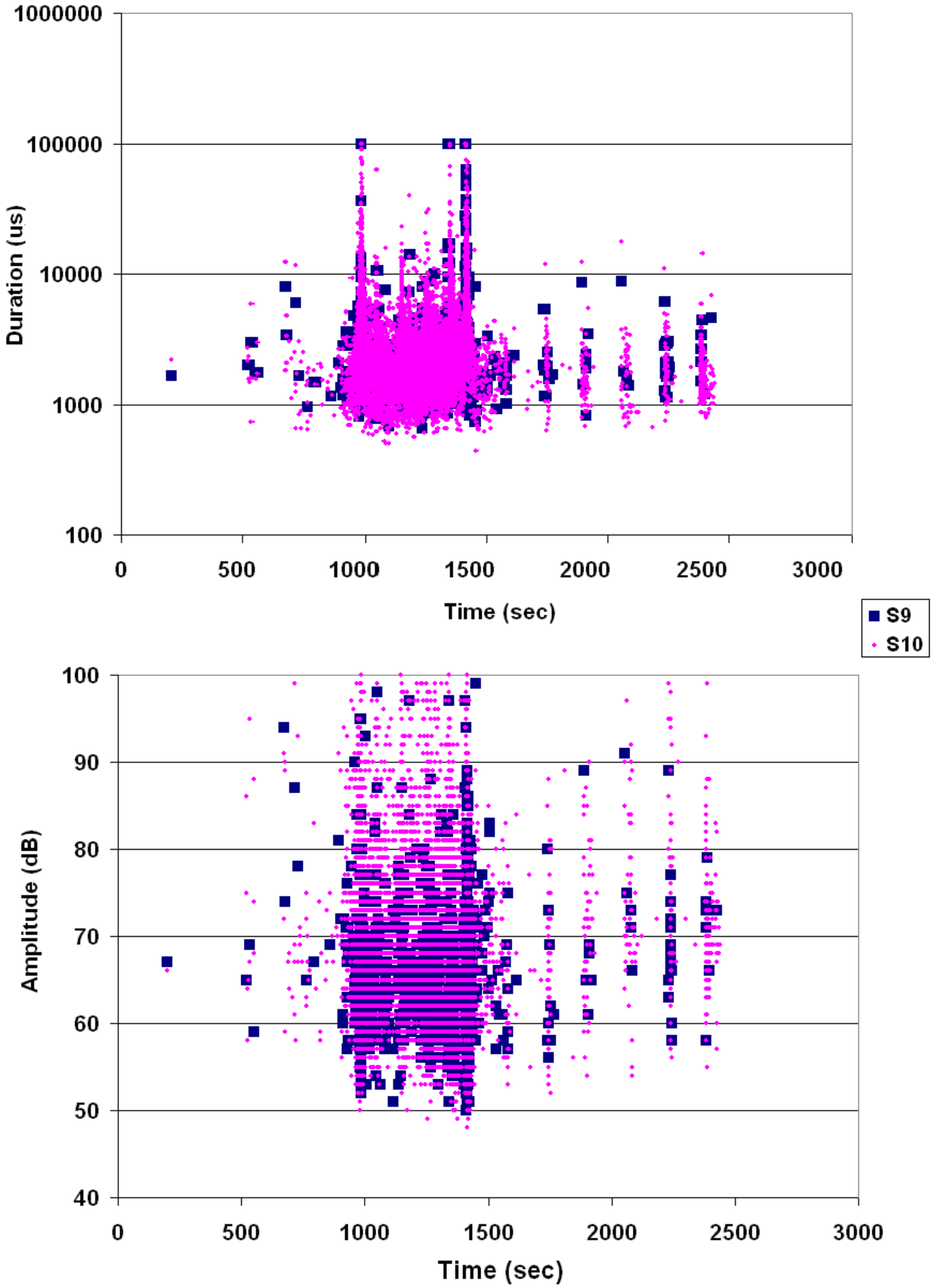

Figure 3-31 Duration and Amplitude comparison of sensors; S9 on top and S10 on bottom.

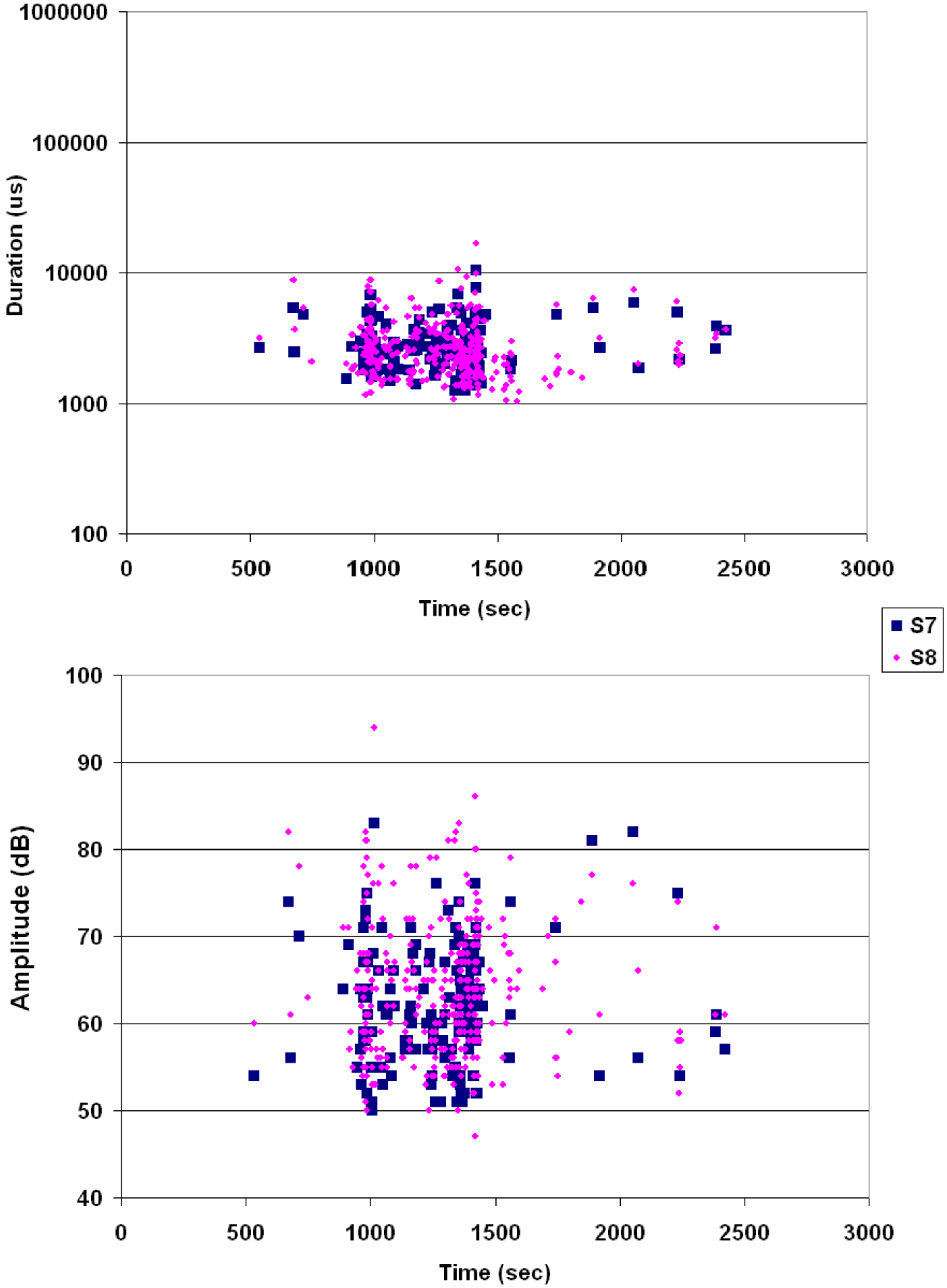

Figure 3-32 Duration and Amplitude comparison of sensors; S7on top and S8 on bottom.

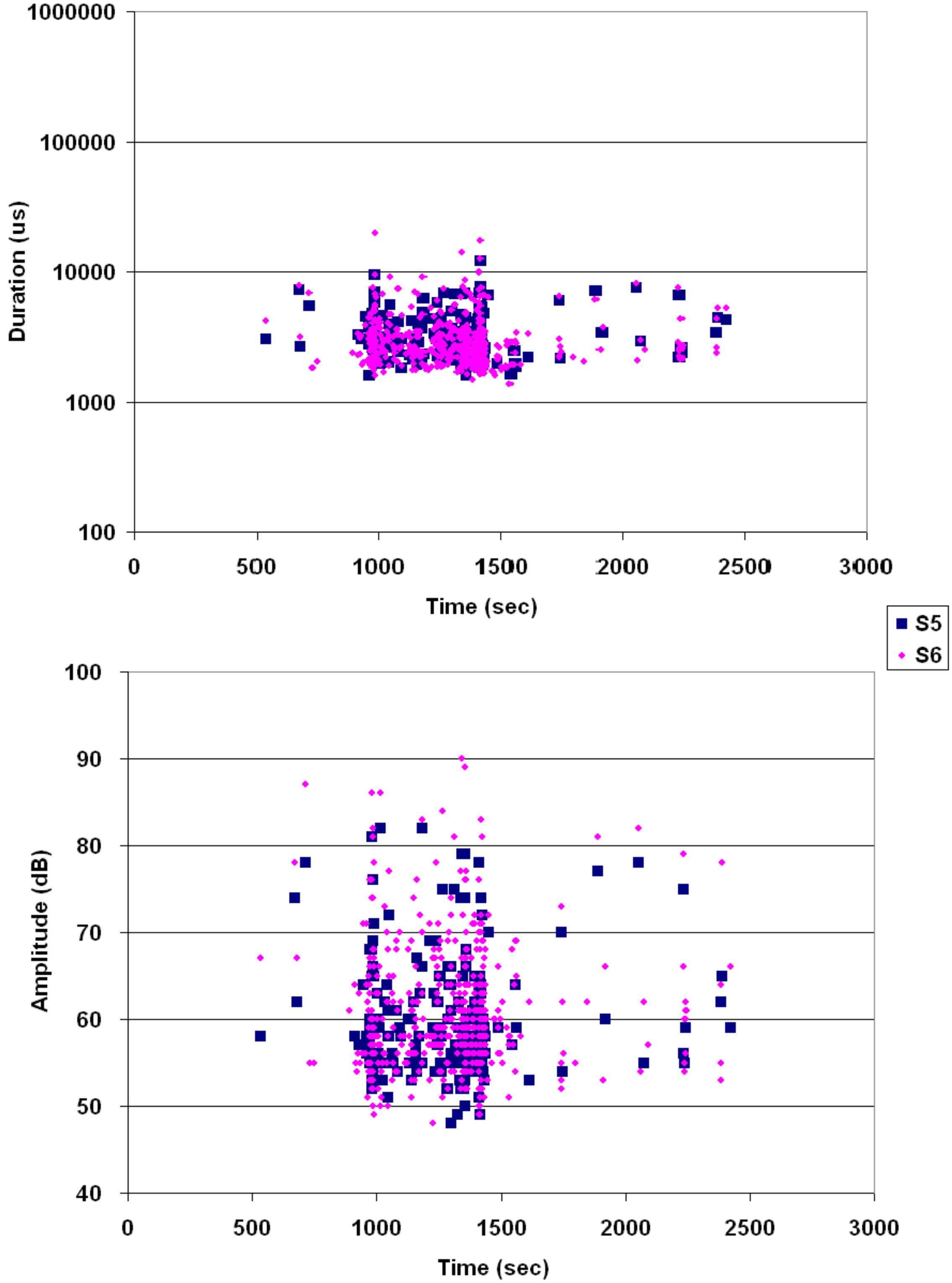

Figure 3-33 Duration and Amplitude comparison of sensors; S5 on top and S6 on bottom.

3.5 Signal transfer in FRP panels

One set of tests focused on analyzing performance along the joint with the force application location, specifically at the middle of the first beam on Panel-A. The sensors were positioned in locations that would result in similar distances from the force being applied, but located on separate panels, as shown in Figure 3-34. By this method a general profile should become apparent as to how well the acoustic data transfers from one panel to the other.

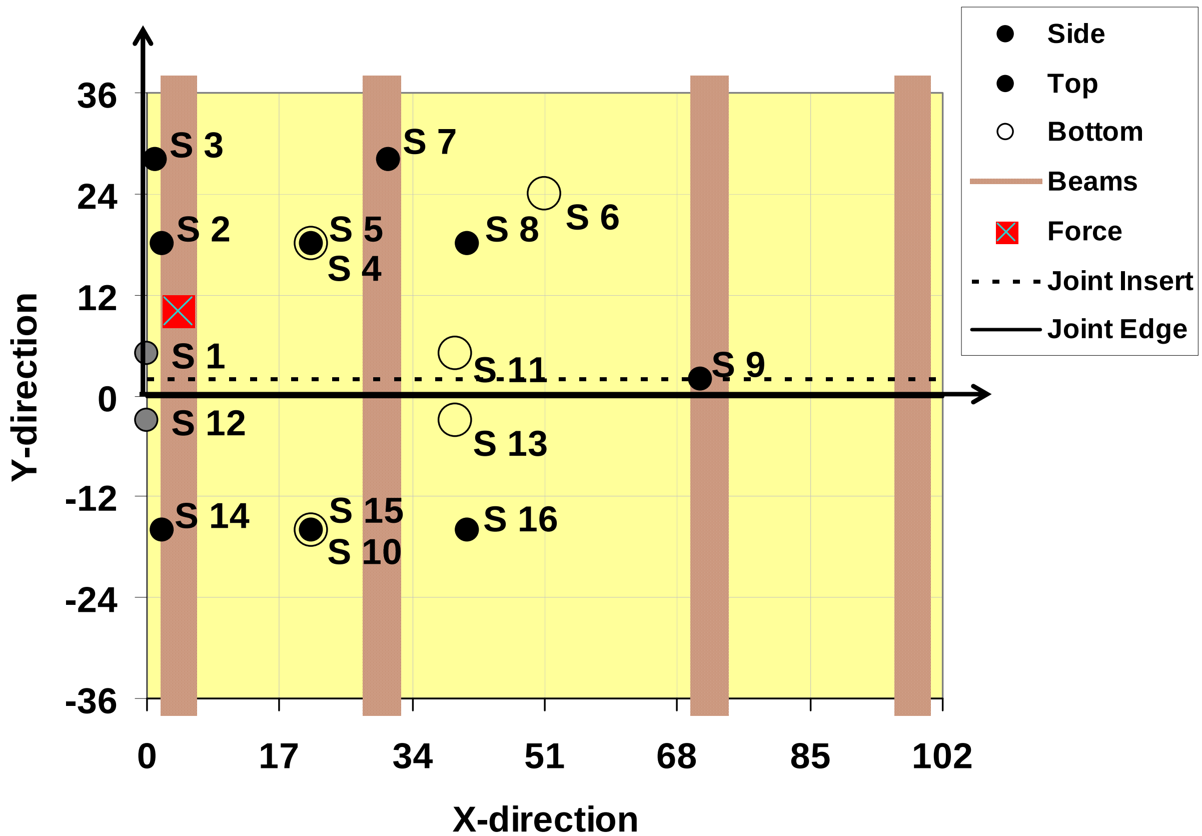

Figure 3-34 Signal Transfer sensor arrangement.

During the setup process the sensor placement was originally intended to record data for a force located on the crack itself. However, upon further planning it was determined this would not work appropriately. The force would cause acoustic data to occur in Panel-B not just due to transfer from Panel-A, but due to a force transfer through the material touching the lip to come under stress and possibly experience some inadvertent bending forces. This would result in a large amount of sensor readings coming from the lip of Panel-B due to the nature of the Lip-and-

Groove connection. Due to multiple likely acoustic source locations the overall effectiveness of the study would be diminished.

Another concern is damaging the panels themselves. While one is eventually damaged at the end of this stage of the project, breaking the panels unnecessarily is not the goal of this investigation. The lip would likely experience bending resulting in damage to that location on the structure, and subsequently cause the joint to need repair before further analyses could be attempted. Additionally, the load could simply break the lip off of Panel-B without an adequate substitution ready to go within a satisfactory time frame.

Instead the load was kept in a location approximately 10 inches from the joint edge, and placed over the first beam. The sensors were then compared to one another based off their general location on the structure over a series of three tests occurring in the same arrangement. For example sensors S7 and S15 are located approximately 32.5 and 31.5 inches from the source and are on separate panels. The resulting graphs would therefore be expected to be similar if the joint does not create a problem for acoustic transfer between the panels. Three other pairs of sensors are located at points that are acceptably the same in distance from the source, having less than two inches of difference. They are S6-S16, S7-S 10, and S11-S13.

The comparison between S6 and S16 is basically non-existent. After the data has been filtered and plotted, there is almost nothing to compare between the sensors. While there is some information that is similar to each other in the S7-S15 comparison, the vast majority of data points graphed do not lead to a good comparison between the sensors. These results are most likely due to the distance between the loading source and the sensor locations, well over two feet away in all cases.

The S7-S10 comparisons have an interesting problem of their own, where the S10 sensor records large amounts of data while the other does not. The sensor designated S15 does not receive as much data as it’s similarly distanced S10 either. The most likely cause for this is that the sensors located on the bottom of the panels, at a moderate distance from the loading source, may be detecting noise created from the panels interacting with the beams they are supported with. This is most likely due to localized matrix cracking and possibly rubbing or movement between the panels and beams. Representative graphs for the S7-S10 comparison in terms of absolute energy and signal strength can be found as Figure 3-35 and Figure 3-36 on the next page.

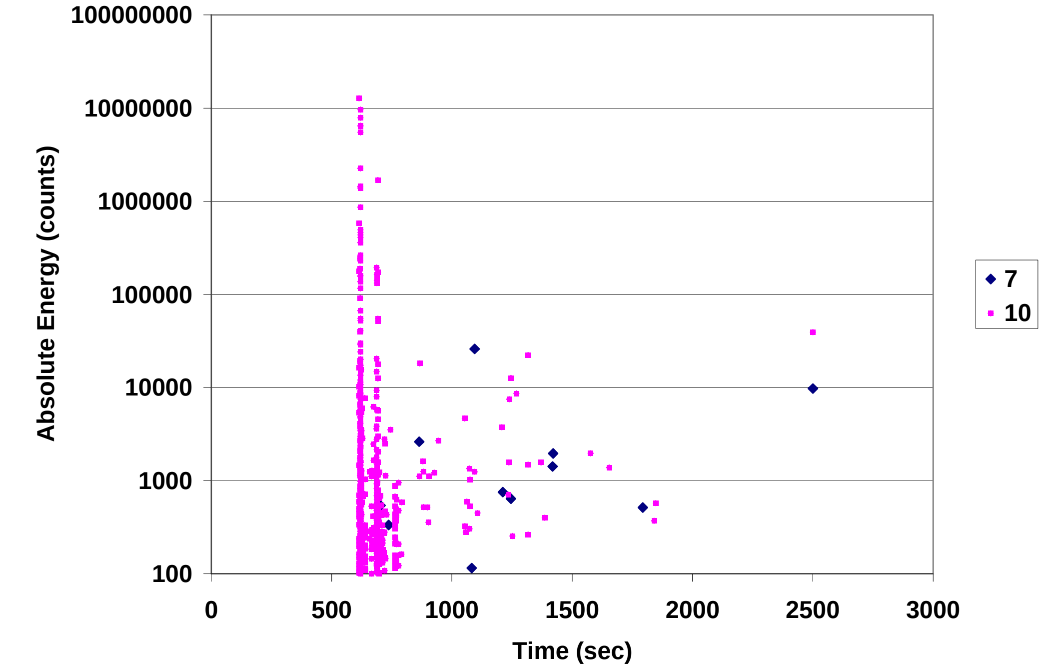

Figure 3-35 Absolute Energy comparison of sensors located equal distances from the source; S7 on top of Panel-A and S10 on bottom of Panel-B.

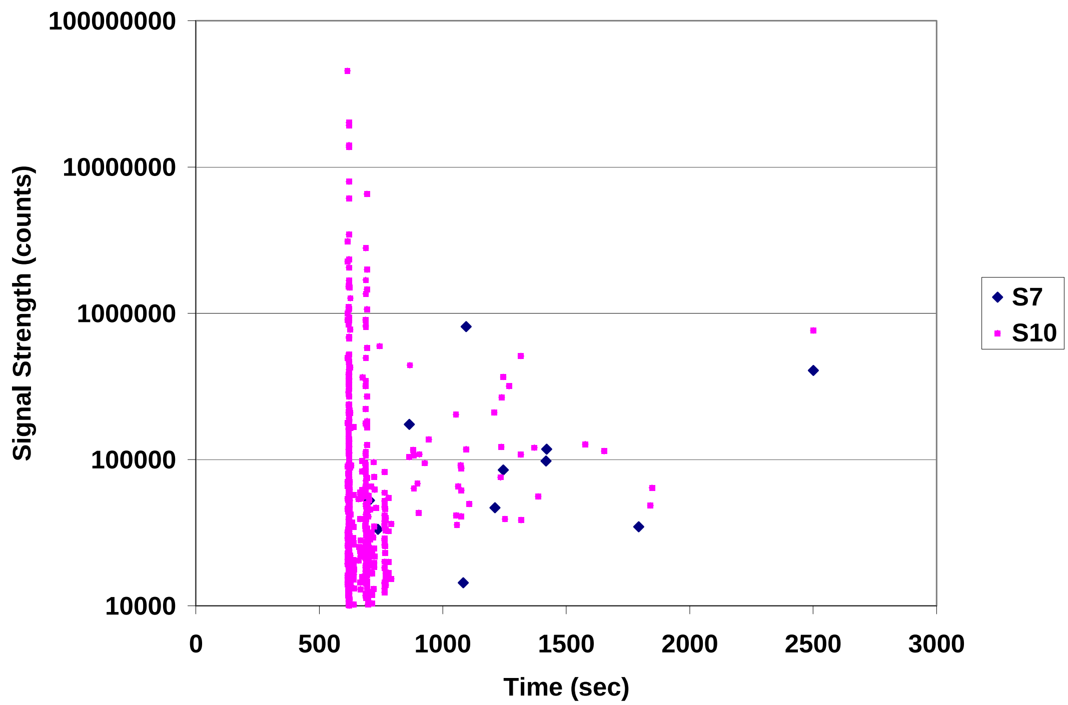

Figure 3-36 Signal Strength comparison of sensors located equal distances from the source; S7 on top of Panel-A and S10 on bottom of Panel-B.

The last set of sensors provides more useful data in which a clearer pattern can be seen in Figure 3-37 below. However, the extreme closeness of the two sensors to one another and proximity to the joint in general may be the overwhelming cause of these results. Any movement experienced between he panels could create an acoustic event, and therefore both panels would transmit the signal through themselves and to the sensors, but not be a transfer from one panel to the next.

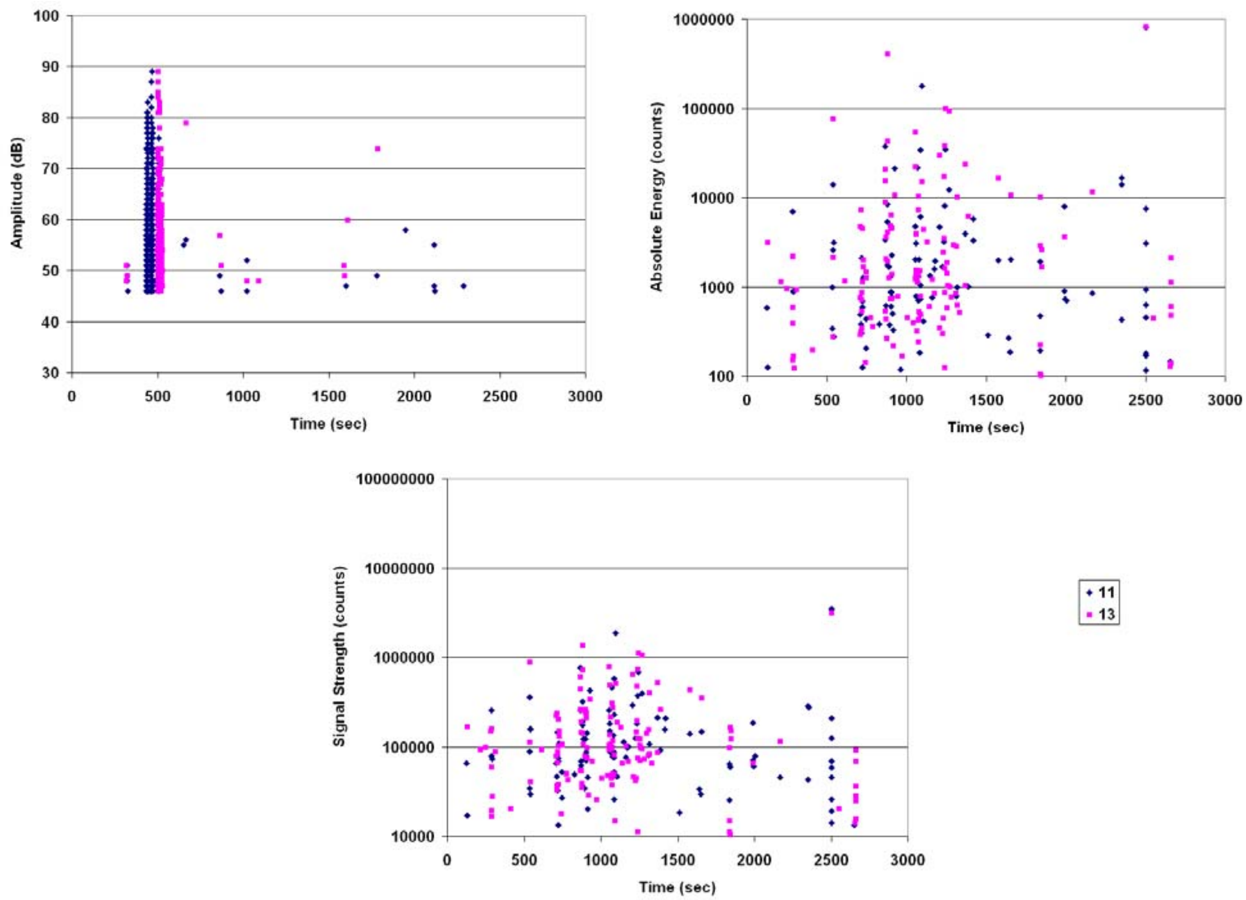

Figure 3-37 Amplitude, Absolute Energy, and Signal Strength comparison of sensors located equal distances from the source; S11 on Panel-A and S13 on Panel-B.

Due to the uncertainty of these results the force location was moved between the first and second beam. This change in location, though short, creates a greater bending force in the panel, and therefore should create more acoustic emissions from material failure. The change in location also makes it so three sensors are spaced approximately the same distance at just over two feet away from the force location. Sensor locations S3 and S8 were located on Panel-A while S15 on Panel-B could be used as the comparison sensor for signal transfer. The resulting graphs show some correlation, indicating that the decrease in distance between the sensors and the loading application point does create readings that are both clearer and more comparable to one another. The graphs below, for amplitude, shows that sensor S15 recorded more data hits than the other two, especially during the start and end of the test during low loads. While some correlation can be seen in the increase and decrease of the values, it is a small one. During higher loading the unloaded panel does have some response, but the magnitudes of these points are far less than those on the loaded panel itself.

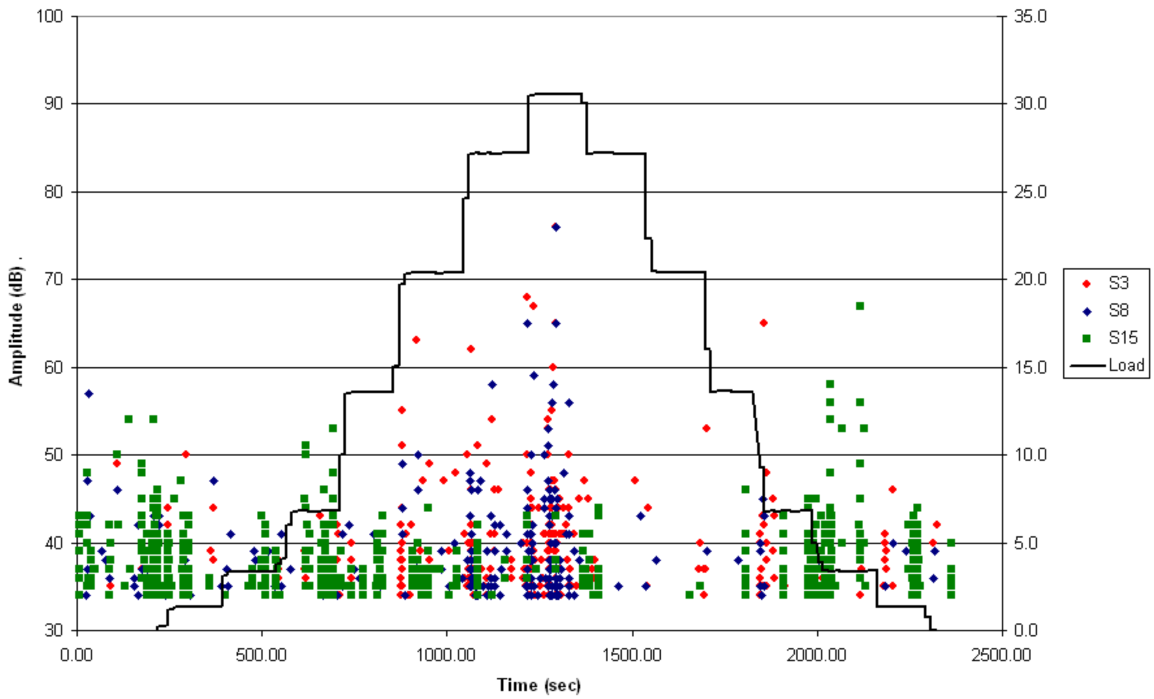

Figure 3-38 Signal Strength comparison of sensors located equal distances from the source; S3 and S8 on Panel-A and S15 on Panel-B.

From the testing results it seems that low load acoustic events can create hit points within both panels; this is most likely due to cracking near the edge of the second panel and not due to an actual signal transfer. Therefore it seems that the sensors on separate panels are more comparable when the sensors are located near each other, and not just at similar distances.

3.6 Single failure event analysis

Towards the end of the run of tests, a one was conducted on the single beam that inadvertently became an opportunity to analyze some failure data for Panel-A's internal structure.

A Single Panel Analysis: Leading to Failure

A force was being applied to the center of the panel, at locations on and between beams located horizontally from the force application point designated in Figure 3-39, which is placed at the location where the failure occurred. The two preceding tests occurred centered over Beams 2 and 3, respectively, but none of the information recorded at the time hinted at the upcoming failure. In fact, there is very little acoustic data at all from the test over Beam 2, even without using the signal strength and energy filters. The test from Beam 3 contained more data but not as much as in earlier tests, indicating that even in this analysis not much took place in regards to acoustically significant events. After the failure occurred an earlier test was reexamined to determine if any earlier signals were present to the oncoming event.

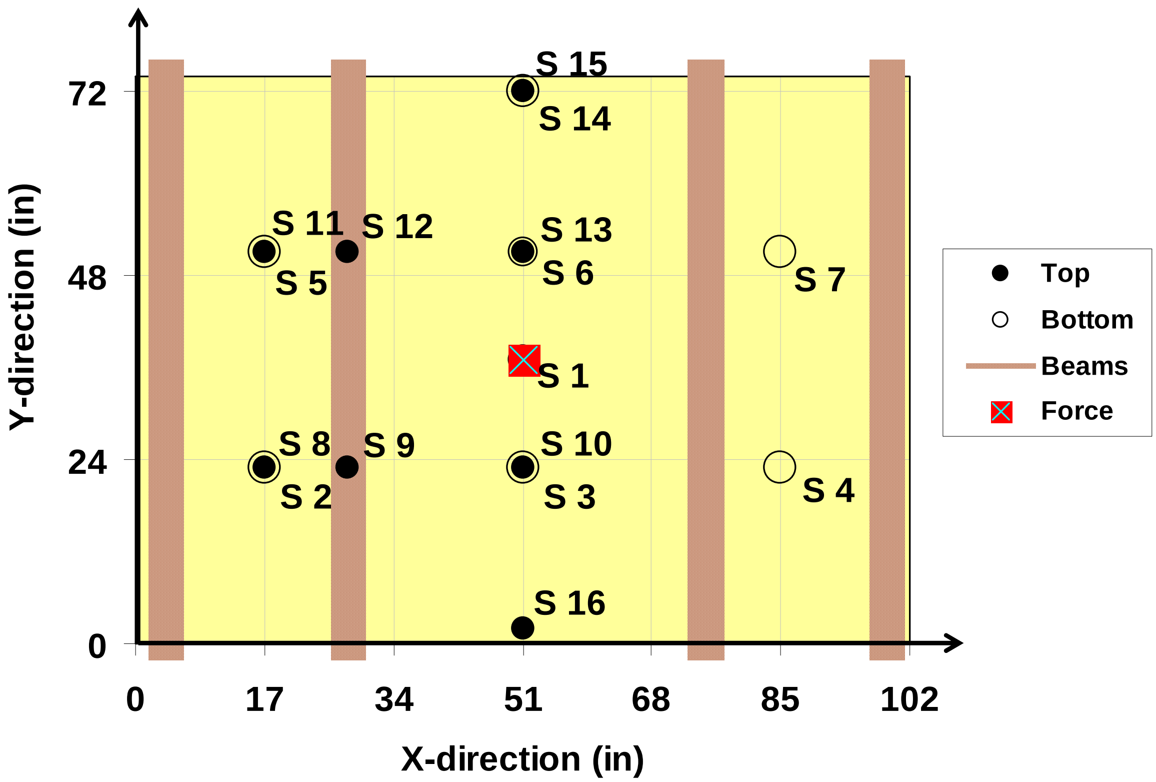

Figure 3-39 Final Sensor Location Layout.

When the hits are plotted on a Duration-Amplitude graph the data from the test over Beam 3, Figure 3-40, the hits barely get into the upper third of the graph, and are predominantly centered in the section designated for low-amplitude matrix failure. There seems to be no indication of fiber failure or any major structural problems by use of this method; however with the beams located under the force application locations the structure is most likely held together more rigidly than it is when the force is between the beams.

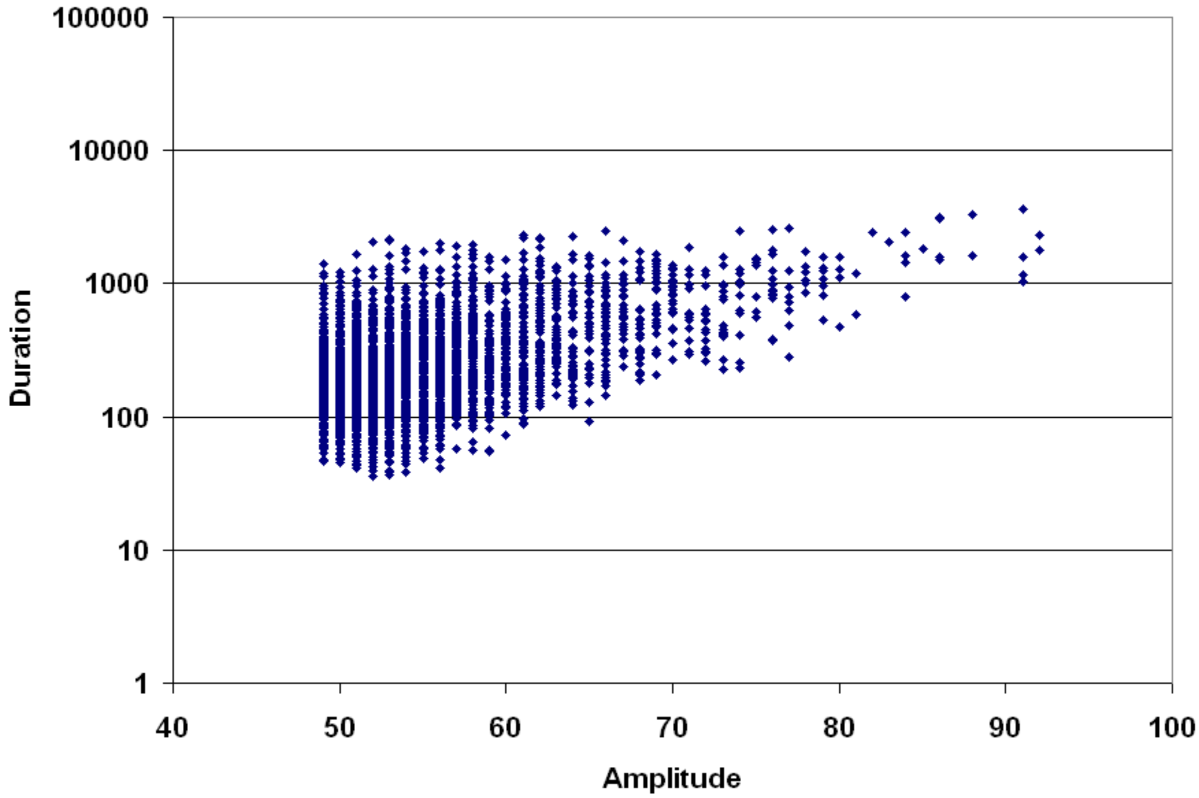

Figure 3-40 Test over Beam 3, Duration-Amplitude graph of all sensors

At this point a closer pre-failure analysis was done on the last test to be conducted between the second and third beams; however this took place only ten inches from the joint edge, not actually at the failure location. Also, the sensors were set up in the configuration presented in Figure 3-18. While there was no analysis performed with sensors located at the failure area prior to the actual failure, and no other test involved the force being applied at the center of either panel used, this data could still give us insight as to if there is any increased risk to having the force applied between the center beams. In Figure 3-41 on the next page, the Duration-Amplitude graph shows that a large amount of the data points, once again mostly located in the 'Matrix Failure' area of the graph, but also has a healthy amount of hit points in the region previously designated for 'Crack Growth,' and seems to come from sensor located closer to the center of the panel in the X-direction.

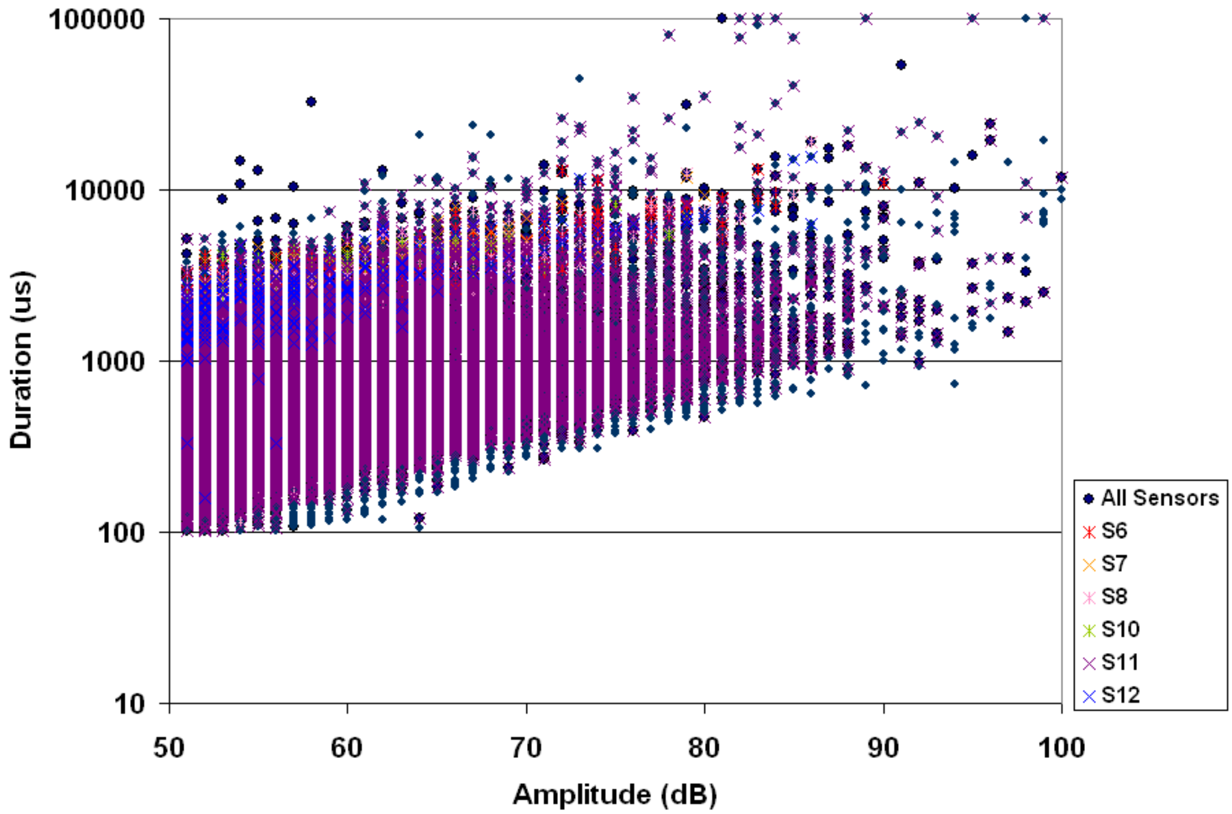

Figure 3-41 Duration-Amplitude Graph of test on the joint edge between Beams 2 and 3.

From this and earlier charts there is some indication that there was little fiber breakage within the structure during the tests regardless of force location. The overwhelming majority of the events seem to indicate that there was some early matrix cracking and growth.

Panel Failure

The initial procedure for the test was conducted similarly to those performed earlier, with a gradually increasing step method. The loading was being applied in steady increments and the peripheral devices were functioning normally. After holding at around twenty kips for approximately two minutes, the load was manually increased until twenty-seven kips was obtained. The load was held steadily for approximately one minute at which time audible sounds began emanating from the structure and a sudden decrease of load occurred. The load then quickly spiked a minute later while the cylinder was being controlled by the user, but was then removed from the structure entirely. The selected loading cycles and amplitude data are presented in Figure 3-42 below, while energy and duration can be found on the next page.

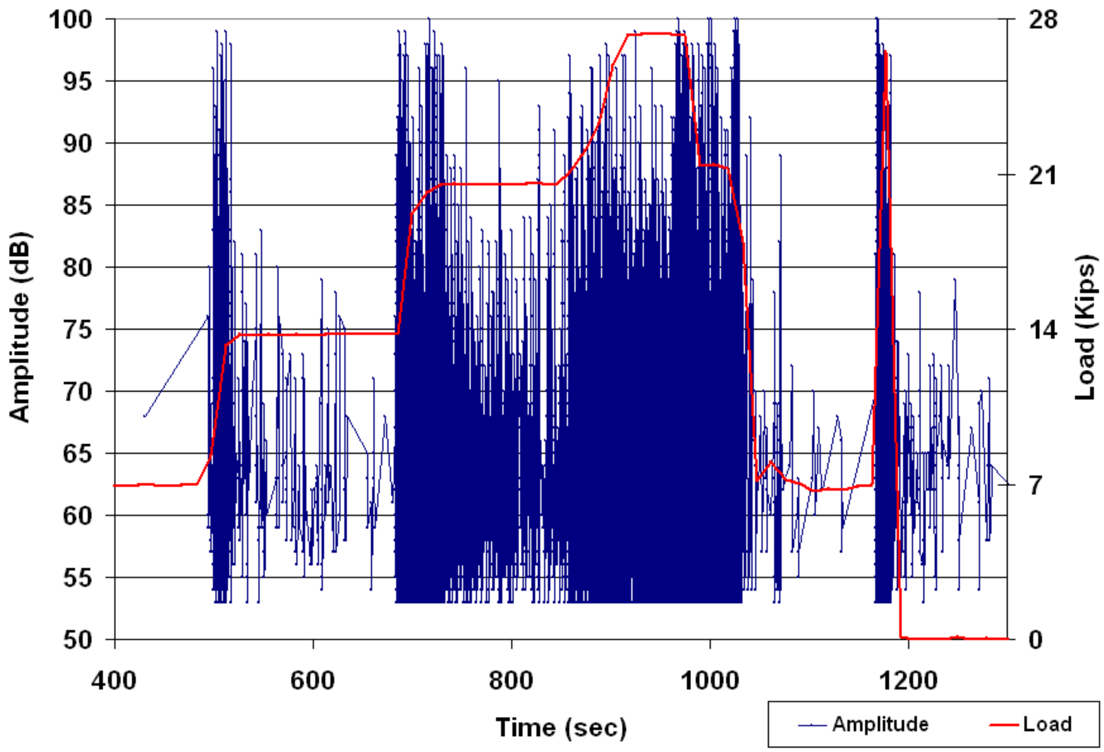

Figure 3-42 Failure during test, Amplitude with Load overlay.

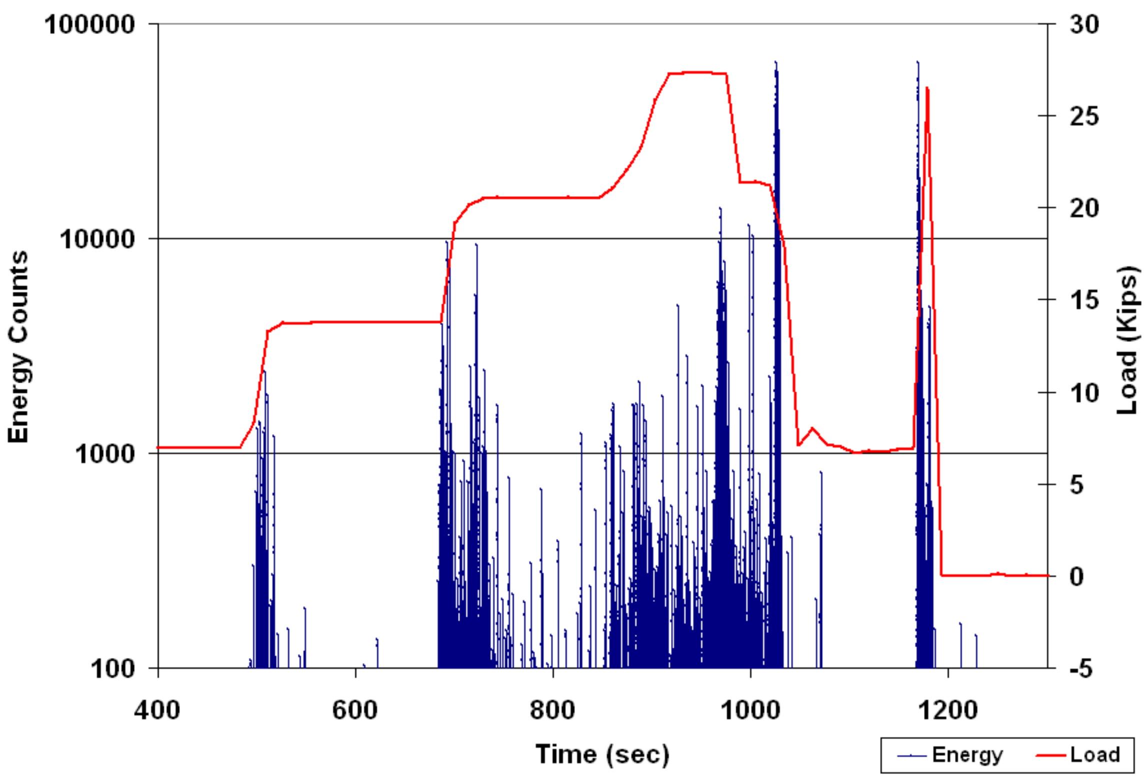

Figure 3-43 Failure during test, Absolute Energy with Load overlay.

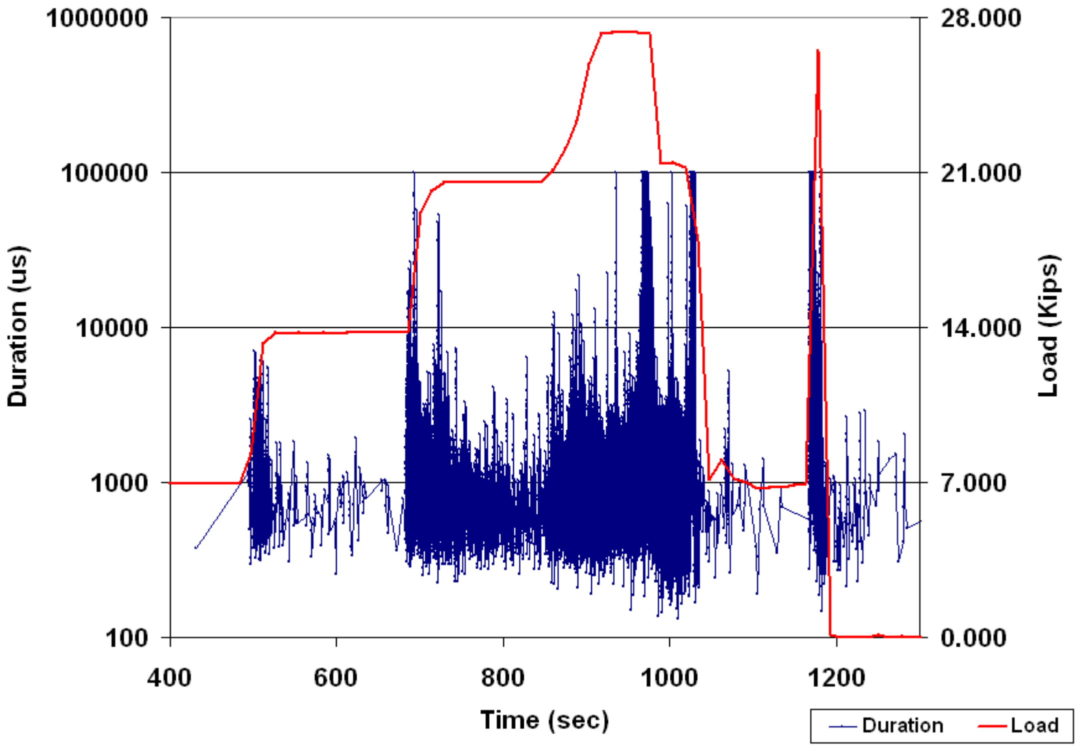

Figure 3-44 Failure during test, Duration with Load overlay.

The cause of the failure was initially unknown and no sign that anything went wrong was noticeable on the exterior of the structure. Subsequent examinations showed that the load likely caused damage to the interior of the panel, a theory which was further supported to when the load was reapplied and the boot actually 'sunk' into the surface of the panel by about an inch when the normal load was applied.

Before the failure occurs there is a significant difference noticeable in terms of the AE property responses during the increase performed before the failure and all earlier increases in load. As can bee seen in the figures related to this test on the previous page, when the load increases there is no sudden spike of activity as has occurred in nearly every examination up to this point. Instead the values slowly increases in response to this new load and does not see nearly as much change in magnitude as was in earlier runs. Upon reaching the new load the property magnitude does not seem to decrease, but remains at about the same amount up until the failure. Another occurrence is that upon reaching the maximum load the magnitudes receded briefly and proceeded to increase again right before the failure occurred.

Another change can be seen in terms of the amplitude. In earlier analyses the magnitude would remain mostly below 80 dB, and rarely exceed 90 dB. However, we can see that prior to the failure event there were several points when the amplitude would spike to nearly 100 dB, and may have been much greater than that value, but was unable to be recorded due to exceeding the recordable range. This occurred each time the load was increased, and after the last load increase we can see the amplitude increased and stayed steady up until the failure occurred, at which point it spiked to the maximum value and remained near this high range until the load was removed from the structure.

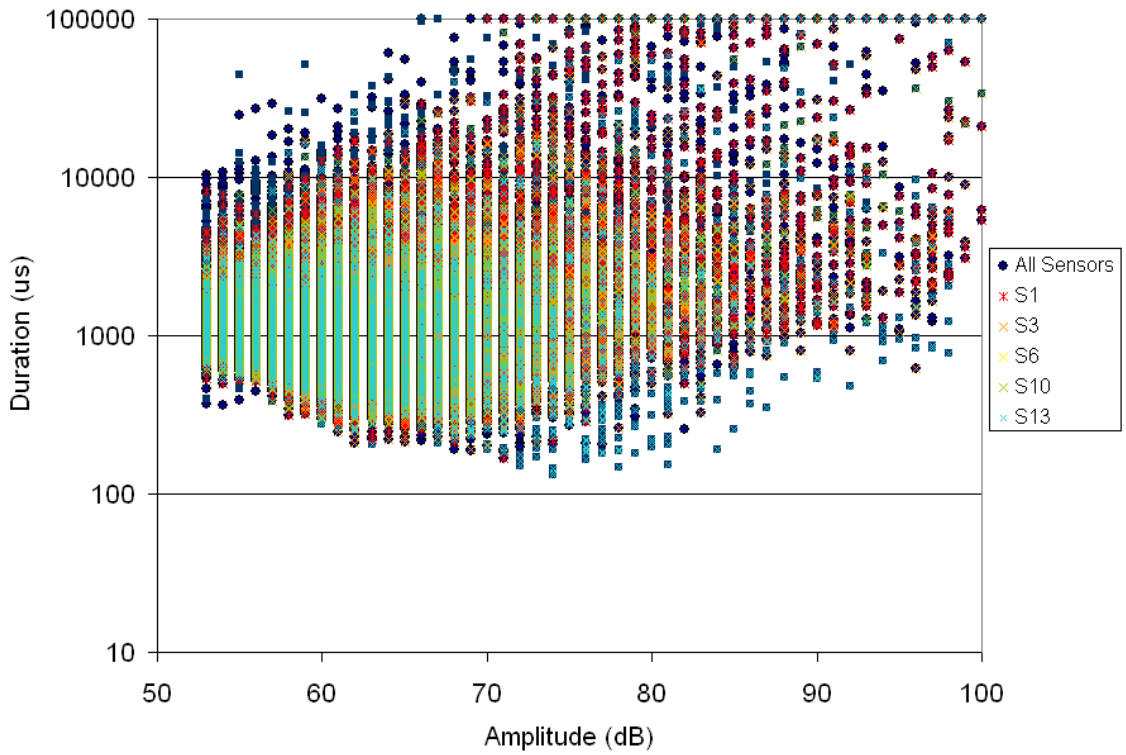

Figure 3-45 Duration-Amplitude plot of the failure test.

From the Duration-Amplitude graph displayed here we can see that there was a large amount of mid-amplitude, high duration hits recorded during the test. As with the analysis of the earlier test conducted between the two interior beams, this has been found to correlate to matrix cracking and delamination between the fiber layers. Also noticeable is a lack of high-amplitude, high duration hits, meaning that the most likely cause of the failure is due to the matrix failing and not fiber breakage.

The individual sensor data on the plot of Figure 3-45 to some extent show that the closer to the event sight the sensor was, the more it recorded 'Fiber Breakage' region failure on the graph. This indicates that while matrix failure occurred in the area around the center of the panel, the majority of the fiber failure was constrained to the epicenter of the event.

If the charted hits are separated differently, it becomes apparent that a large amount of the data collected occurred when the applied load reached its maximum value creating a resulting stress that caused the matrix to cracks and the overall structure to fail. The figure below implies that during the maximum load a concentration of acoustic data is once again formed in the center of the graph designated as 'matrix cracking' and 'crack growth.' These displays imply that the majority of the acoustic data occurred during the maximum loading cycle prior to a failure, most likely due to an overall matrix failure near the load source. Many of the hits in the fiber breaks region apparently occurred during or after the main failure; most likely due to structural collapse of the core material discussed, providing interior structural support.

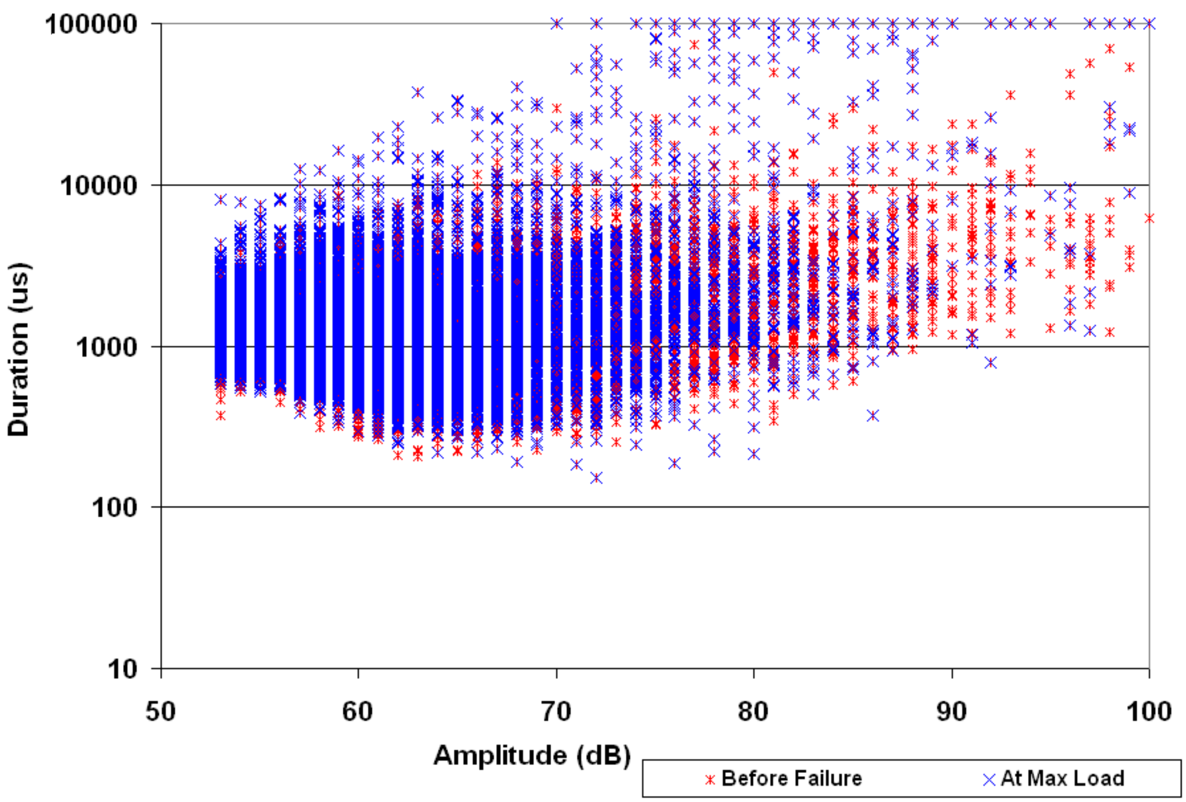

Figure 3-46 Pre- and Post-failure Duration-Amplitude plot of the failure test.

3.7 Long term monitoring

In preparation for the next stage the groundwork was started in making this system completely wireless so that long term monitoring can be conducted without the need to go to the monitoring site to gather the data. In order to make the system more flexible in its application and use the monitoring device will not use a hard-line phone or power lines. The lack of wiring should allow the system to be placed in nearly any location on a bridge structure. The power requirements for the system and the modem are planned to be generated by use of solar energy and a regular car battery storage cell as shown below in Figure 3-47.

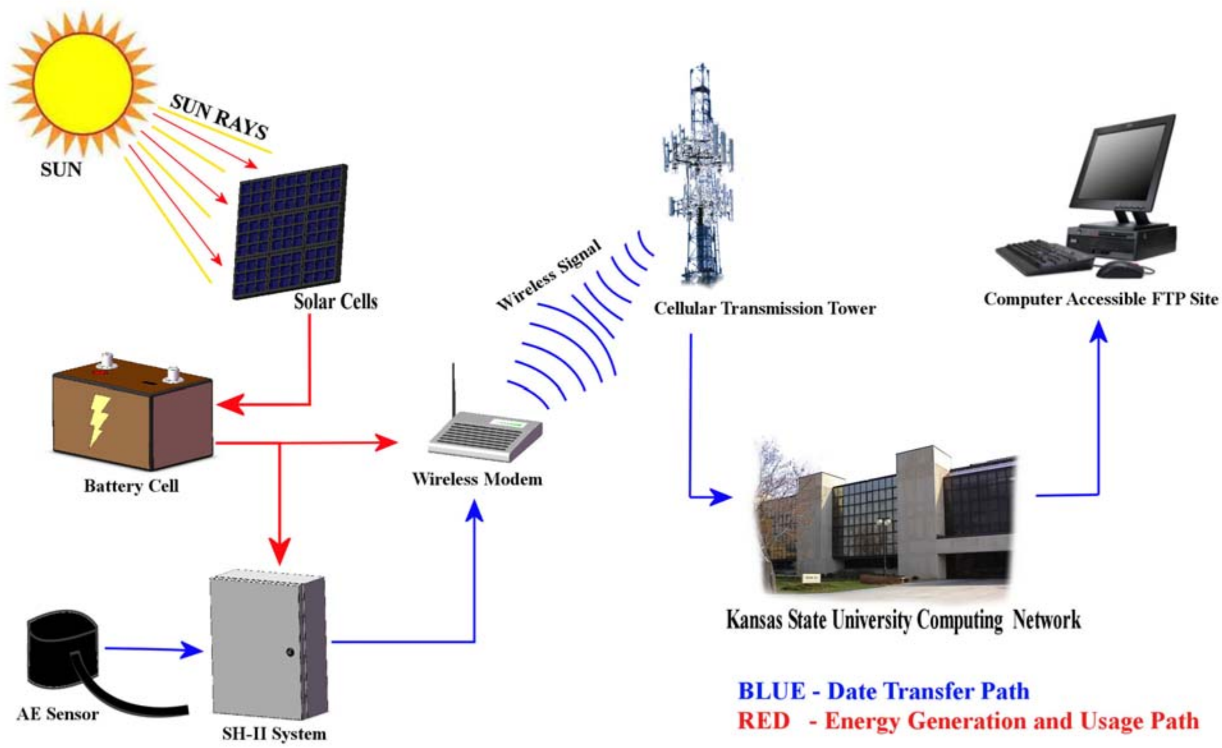

Figure 3-47 Monitoring system's power and data flow chart

The data transfer will be conducted through use of a modem that has been integrated into the SH-II system itself. Upon data collection and applying the filtering process the data will be stored in the flash memory until a designated time each day when the contents will be sent to Kansas State for processing. At a designated time, most likely to be late-night, the system will 'dial up' access to the internet and access a secure FTP site on K-State's campus. Upon contacting the site the contents will be uploaded from the system, subsequently purged from the FC's memory and disconnects from internet access. At this point the system has performed all necessary duties for data upload and continues to record data as normal until the next uploading time. The system can be set up so that if a connection cannot be made for whatever reason the system will not delete the data, but retain it until the next uploading cycle is reached.

The data can be stored on a FTP site on the Kansas State Computing Network, and since this is a secure network the files are at little risk of being accessed, deleted or tampered with by other means from outside sources. This also means the only way to access the data is from on K-State's Manhattan campus, and while this option still has it's limitations it is much more practical than manually downloading the data from the System directly.

CHAPTER 4 SUMMARY AND FUTURE OF RESEARCH

4.1 Summary

From the summer of 2007 to the spring of 2008, tests and analyses were performed on FRP bridge decks at Kansas State University. The applied specimens consisted of two panels of equal size and structure with acoustic sensors and strain gauges attached in various locations to detect loading effects. A variety of properties and sensor presets were used to determine how the sensors should be used in future FRP panel analyses and similar applications. The gathered data consisted of a variety of results and provided significant insight into how the panels would function and possible fail in actual use.

Based on the analyses conducted during this projects a variety of conclusions can be made from the results determined and included in this report. These include:

1. While not initially intended to be tested for, the majority of the results show that the panel is capable of resisting long term damage if a load over 30 kips occurs for at least a short period of time. However, repeated occurrences may have affected the interior structure and eventually lead to localized failure.
2. Thresholds are necessary to keep unwanted data from being recorded. This includes machinery and environmental background noise which seems to usually occur below 45 dB. The analyses showed that additional thresholds could be applied without sacrificing important data, including up to a 60 count energy threshold.
3. The Amplitude-Duration Graph does seem to work well in categorizing the data in terms of what caused the acoustic signal and showed that there were definite regions as to where different types of source failures show up on the plot.
4. Panel failure type can be, at least in part, determined by use of the Duration-Amplitude graph, by looking at what region has more acoustic activity occurring at the time.
5. When a load is first applied it results in increased magnitudes of a amplitude, energy and signal strength. These values quickly decrease after the desired

load has been achieved, but do not return to the earlier values. Instead they remain at an increased state until the load is decreased, at which point a smaller spike in magnitudes sometimes occurs but it then drops as expected with load.

6. Repeated loading cycles occurring in the same panel locations show there is a decreased magnitude in reference to the values displayed during dynamic loading changes, while static loads appear to have similar values in each analysis.
7. Individual sensors have a range of up to two feet for gathering acceptable data. The decrease in property values appears to have an inverse correlation to distance as well as being a second order relationship. This is similar to the activity of past analyses and the overall accepted behavior of acoustic related properties, which equations seem to be typically based on inverse second order equations.
8. While acoustic data does travel through the joint it is unclear how much it affects the signal. The limit of a sensor to be within two feet of the source makes it difficult to examine this property more. This is due to the increase in acoustic signals recorded due to plates contact effects in the sensor is hear the joint or the creation of signals created in both panels when the force applied is near the joint. These problems make it difficult to accurately gauge the signal transfer from one panel to the next.
9. Sensors placed on the underside of the panels can accurately record the data produced in comparison to the sensors on top. There is typically a marginal increase in acoustic activity detected by the bottom sensors, most likely due to the support beams.
10. The most likely form of panel failure will occur in the form of matrix failure from within the structure. When a force is applied the inner layers most likely buckle and fail through means of matrix failure and compressive forces.

4.2 Future Work

The way in which a panel fails still needs to be examined more closely. In previous projects the goal has been to design a panel that could handle bending loads and further the ability of a FRP panel to work under higher loadings. In this project the failure properties of the previously designed structure was touched upon briefly and by accident. A detained examination of what signals are produced prior to and during a failure should be conducted to help predict a failure before it happens.

While the classifications on the Duration-Amplitude graph developed in the earlier project stage seem to be generally accurate, a more detailed could also be performed. This would provide the monitoring personnel a better understanding of what is happening on, and more importantly, in the panel structures.

Additional studies should be conducted into the thresholds applied to the sensors. While some have been utilized in this project, there are most likely more exact values and properties that could be utilized to increase the proficiency and efficiency of the monitoring device.

While a signal location property of the software was utilized in this project it was not utilized to a great extent or included in this report due to the production of obvious results. Due to the nature of the testing procedure used the acoustic source location nearly always related back to the sensor nearest to the force application location. While this is good, and shows that it works properly there are no alternate possible sources anywhere on the structure. If there was a possible way to load on multiple locations it might be interesting to research how the structure responds and how the location software performs in such a situation.

In relation to that, before these sensors are used on an actively used traffic bridge it might be a good idea to apply loads that reflect that environment more. For instance developing a testing setup that would have a 'driven load' wheel go across the surface to determine what effects a dynamic load might have. The location program could then be tested in an environment that has an increased number of properties and determine where 'problem areas' might be located on the surface as a vehicle travels over a panel.

An analysis as to how the beams interact with the panel structure could provide insight into how the distances between the support beams effects the acoustic data and the bridge structural capabilities as a whole. This is only mentioned due to the lack of any failure characteristics being present between the first and second beam in comparison to Beam-2 and

Beam-3, which were farther apart and between which the failure occurred. These locations are also suggested to be where the sensors should be closely monitoring the panels. The bending stresses created by a downward force, in addition to being the more weakly supported section of the panel overall, makes these locations a more likely target for failures to occur.

Sets of arrays in two directions would also help in locating problem areas. While two arrays were able to locate a relative position in the X-direction, having arrays in the Y-direction would most likely yield similar results. These two sets of information together would be very useful in narrowing down the failure location to within a few feet on panels of the size used in this analysis stage.

Finally, when the analyses are being conducted on the bridge, the data should initially be compared on a daily basis to examine what changes occur while the bridge is settling. As shown earlier, a panel seems to change in regard to its acoustic profile as loads are applied and removed. And while it is impossible to know exactly what loads are being applied to the panels on an active traffic bridge, they will change in terms of the acoustic data produced. The data itself could be compared on increments that start off small, daily or hourly and gradually increase. After a time elapses and the data shows a more constant pattern between comparisons than it may be able to be compared on larger increments. This will allow for small changes to be examined without taking up a large part of the researcher’s time. However, the data from the monitor should still be examined on normal short intervals to look for any hits or events that are unusual as they may be an indication of a sudden incident of activity.

Glossary

Amplitude: The peak voltage value measured during an individual hit. These values are typically measured in decibels (dB).

Duration: The time during which an individual hit's voltage is recorded from start to the amplitude and back down. These values are usually recorded in μs.

Energy: Sometimes referred to as Energy Counts or MARSE. MARSE is an acronym standing for Measured Area of the Rectified Signal Envelope. This is referring to the area under the curve of a Voltage, or amplitude, chart. This takes into account both the Amplitude and Duration of a hit, which are both used heavily in acoustic emission studies. This allows for the two properties to be combined and more easily compared with other hits in the same or separate events. These values are usually recorded in counts. Physical Acoustics has stated each count is approximately equal to $10x10^{-6}$ V-s.

Event: Each actual acoustic emission that comes from a source. These can result in multiple hits being recorded at the sensor locations.

Hits: Each acoustic signal that occurs over the thresholds, natural or user defined, and can be recorded from a sensor.

Source: The location of the acoustic emission in the structure. This is assumed to be at or near the loading location.

Strength: Intensity of an acoustic wave. Physical Acoustics has stated each count is approximately equal to $3.05x10^{-12}$ V-s.

References

BRE and Trend 2000 Ltd. (2001). Polymer Composites as Construction Materials. Retrieved June 21, 2008, from www.polymercomposites.co.uk/pdf/Bridges.PDF

Ely, Thomas M., and Eric V. K. Hill. “Characterization of Longitudinal Splitting and Fiber Breakage in Graphite Epoxy Using Acoustic Emission Data.” *Materials Evaluation*, February 1996.

Feng, Peng, Leiping Ye, Tianhong Li, and Qianli Ma. "Outside Filament-wound Reinforcement: A Novel Configuration for FRP Bridge Decks." The Ninth International Symposium on Dtructural Engineering for Young Experts. Fuxhou & Xiamen, China, (August 18-21 2006)

Gostautas, Richard S., Guillermo Ramirez, Robert J. Peterman, and Dave Meggers. "Acoustic Emission Monitoring and Analysis of Glass Fiber-Reinforces Composites Bridge Decks." Journal of Bridge Engineering NoDe (2005): 713-721.

Kowalik, Alan. Acoustic Monitoring on the Fred Hartman Bridge. Bridge Division, Texas Department of Transportation. Retrieved 15 Jan. 2008 from www.dot.state.tx.us/ publications/bridge/hartman_acoustic_monitoring.pdf

Kawamoto, Sumire, and R. Sam Williams. Acoustic Emission and Acousto-Ultrasonic Techniques for Wood and Wood-Based Composites. United States. Forest Service, Forest Products Laboratory. Department of Agriculture. Jan. 29, 2003.

KSCI (2007). Kansas Structural Composite, Inc. website. Retrieved January 30, 2008, from www.ksci.com/frpbridges.html

Liu, Wingi. Response of No-Name Creek FRP Bridge to Local Weather. May 1, 2006. Dept. of Mechanical Engineering Kansas State University. Prepared for Kansas Department of Transportation (A Report)

McWilliam, Fiona (July 21, 1994). Building Bridges from Old to New. Retrieved June 21, 2008, from www.contractjournal.com/Articles/1994/07/21/30679/ building-bridges-from-old-to-new.html

Prine, David W. Application of Acoustic, Strain, and Optical Sensors to NDE of Steel Highway Bridges. Sensors Expo Conference, 16 May 1995, BIRL Industrial Research Laboratory, Northwestern University. Retrieved 15 Jan. 2008 from www.iti.northwestern.edu/ publications/technical_reports/tr12.html

Sison, Miguel, J.C. Duke, Jr., G. Clemeña, and M.G. Lozev. Acoustic Emission: A Tool for the Bridge Engineer. 1996, The American Society for Non-Destructive Testing. Retrieved 7 June, 2008 from http://www.asnt.org/publications/materialseval/solution/augustsolution/ augustsolution.htm

Uppal, A. Shakoor. "Monitoring Bridge Components Using Acoustic Emissions." Railway Track and Structures Sept. (2000). Retrieved 15 Jan. 2008 from www.findarticles.com/p/ articles/mi_m0BFW/is_9_96/ai_66121906

Walker, JamesL., Gary L. Workman. "Study Acoustic Emissions from Composites." NASA Final Draft Report (December, 1997): 713-721.

Zhou, Eric, Youqi Wang, David Meggers, and Jerry Plunkett. “Field Tests to Determine Static and Dynamic Response to Traffic Loads of Fiber-Reinforced Polyester No-Name Creek Bridge,” *Transportation Research Record*: Journal of the Transportation Research Board, No. 2028, 2007, pp. 231-237.